

## Evaluation of the rhenium–osmium geochronometer in the Phosphoria petroleum system, Bighorn Basin of Wyoming and Montana, USA

Paul G. Lillis<sup>a,\*</sup>, David Selby<sup>b</sup>

<sup>a</sup> U.S. Geological Survey, Box 25046, MS 977, Denver Federal Center, Denver, CO 80225, USA

<sup>b</sup> Department of Earth Sciences, Durham University, Durham DH1 3LE, UK

Received 21 August 2012; accepted in revised form 19 April 2013; available online 1 May 2013

### Abstract

Rhenium–osmium (Re–Os) geochronometry is applied to crude oils derived from the Permian Phosphoria Formation of the Bighorn Basin in Wyoming and Montana to determine whether the radiogenic age reflects the timing of petroleum generation, timing of migration, age of the source rock, or the timing of thermochemical sulfate reduction (TSR). The oils selected for this study are interpreted to be derived from the Meade Peak Phosphatic Shale and Retort Phosphatic Shale Members of the Phosphoria Formation based on oil–oil and oil–source rock correlations utilizing bulk properties, elemental composition,  $\delta^{13}\text{C}$  and  $\delta^{34}\text{S}$  values, and biomarker distributions. The  $\delta^{34}\text{S}$  values of the oils range from  $-6.2\text{‰}$  to  $+5.7\text{‰}$ , with oils heavier than  $-2\text{‰}$  interpreted to be indicative of TSR. The Re and Os isotope data of the Phosphoria oils plot in two general trends: (1) the main trend ( $n = 15$  oils) yielding a Triassic age ( $239 \pm 43$  Ma) with an initial  $^{187}\text{Os}/^{188}\text{Os}$  value of  $0.85 \pm 0.42$  and a mean square weighted deviation (MSWD) of 1596, and (2) the Torchlight trend ( $n = 4$  oils) yielding a Miocene age ( $9.24 \pm 0.39$  Ma) with an initial  $^{187}\text{Os}/^{188}\text{Os}$  value of  $1.88 \pm 0.01$  and a MSWD of 0.05. The scatter (high MSWD) in the main-trend regression is due, in part, to TSR in reservoirs along the eastern margin of the basin. Excluding oils that have experienced TSR, the regression is significantly improved, yielding an age of  $211 \pm 21$  Ma with a MSWD of 148. This revised age is consistent with some studies that have proposed Late Triassic as the beginning of Phosphoria oil generation and migration, and does not seem to reflect the source rock age (Permian) or the timing of re-migration (Late Cretaceous to Eocene) associated with the Laramide orogeny. The low precision of the revised regression ( $\pm 21$  Ma) is not unexpected for this oil family given the long duration of generation from a large geographic area of mature Phosphoria source rock, and the possible range in the initial  $^{187}\text{Os}/^{188}\text{Os}$  values of the Meade Peak and Retort source units. Effects of re-migration may have contributed to the scatter, but thermal cracking and biodegradation likely have had minimal or no effect on the main-trend regression. The four Phosphoria-sourced oils from Torchlight and Lamb fields yield a precise Miocene age Re–Os isochron that may reflect the end of TSR in the reservoir due to cooling below a threshold temperature in the last 10 m.y. from uplift and erosion of overlying rocks.

The mechanism for the formation of a Re–Os isotopic relationship in a family of crude oils may involve multiple steps in the petroleum generation process. Bitumen generation from the source rock kerogen may provide a reset of the isotopic chronometer, and incremental expulsion of oil over the duration of the oil window may provide some of the variation seen in  $^{187}\text{Re}/^{188}\text{Os}$  values from an oil family.

© 2013 The Authors. Published by Elsevier Ltd. Open access under [CC BY-NC-SA license](https://creativecommons.org/licenses/by-nc-sa/4.0/).

\* Corresponding author. Tel.: +1 303 236 9382; fax: +1 303 236 3202.

E-mail addresses: [plillis@usgs.gov](mailto:plillis@usgs.gov) (P.G. Lillis), [david.selby@durham.ac.uk](mailto:david.selby@durham.ac.uk) (D. Selby).

### 1. INTRODUCTION

Rhenium–osmium (Re–Os) geochronology has been successfully developed to ascertain the depositional age of organic-rich sedimentary rocks (Ravizza and Turekian, 1989; Cohen et al., 1999; Creaser et al., 2002; Selby and Creaser, 2005a; Kendall et al., 2009a,b; Xu et al., 2009; Rooney et al., 2010, 2011; Georgiev et al., 2011; Cumming et al., 2012). The application of Re–Os geochronology to crude oil and solid bitumen deposits has yielded ages interpreted to reflect the timing of oil generation or migration (Selby and Creaser, 2005b; Selby et al., 2005; Finlay et al., 2011). However, we do not fully understand the elemental and isotopic behavior of Re and Os in the transfer from source rocks to petroleum, although hydrous pyrolysis experiments of source rocks have provided some insights into the process (Rooney et al., 2012). Previous Re–Os crude oil and bitumen studies have investigated hydrocarbons that are weakly to heavily biodegraded and suggest

that biodegradation does not affect the Re–Os systematics in petroleum (Selby and Creaser, 2005b; Selby et al., 2005). However, the effects of other secondary processes, such as thermal cracking and thermochemical sulfate reduction (TSR) on Re–Os systematics in petroleum have not been established.

In this study we apply Re–Os geochronometry to crude oils of the Permian Phosphoria petroleum system from the Bighorn Basin in Wyoming and Montana (Fig. 1), to determine whether the radiogenic age reflects the timing of petroleum generation, timing of migration, age of the source rock, or the timing of secondary petroleum alteration, with a particular focus on the effects of TSR.

### 2. GEOLOGY OF THE PHOSPHORIA PETROLEUM SYSTEM

Petroleum derived from the Permian Phosphoria Formation occurs in Wyoming, Montana, Colorado, and

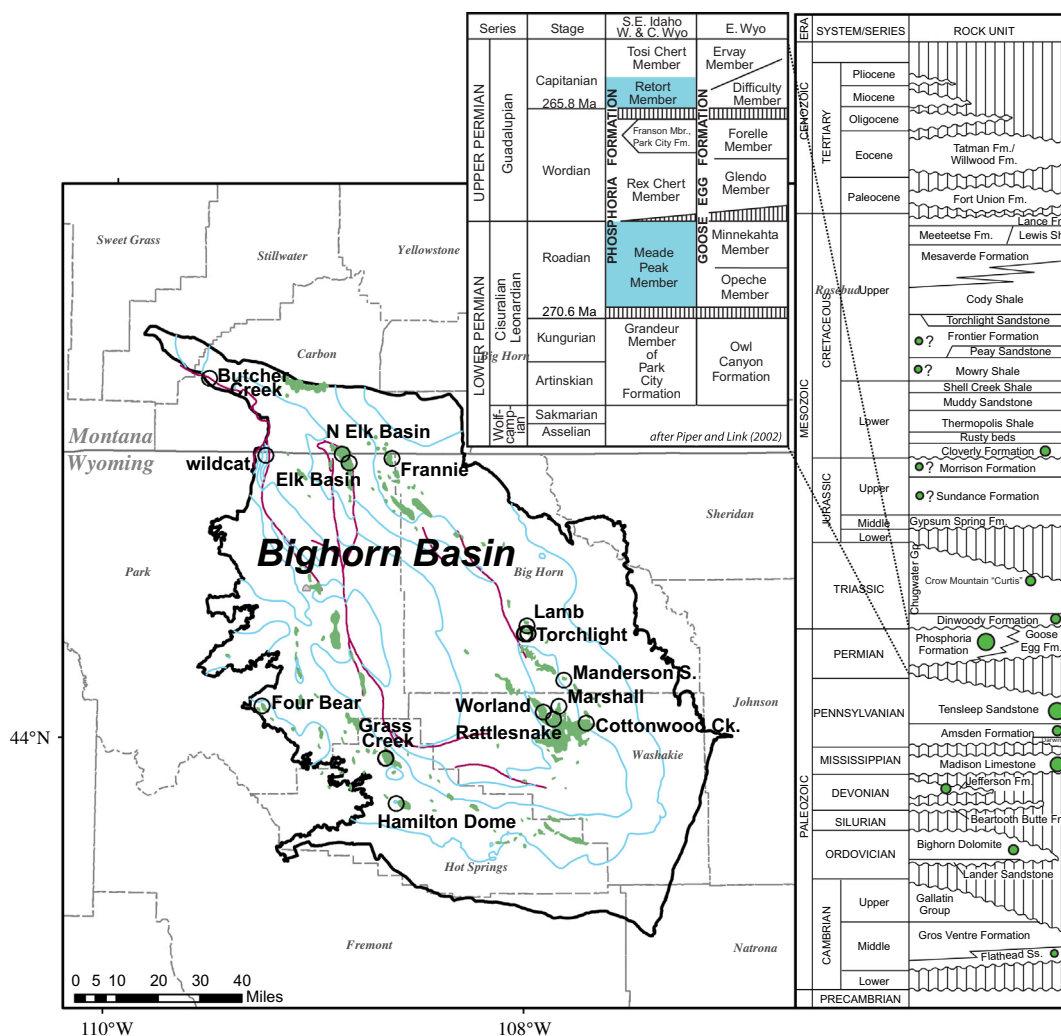


Fig. 1. Map of the Bighorn Basin showing oil sample locations (open circles), oil fields (green), basin outline, top of Cloverly Formation structure contours (5000 ft intervals), major faults (red), and county boundaries (Kirschbaum et al., 2008; Roberts et al., 2008). Stratigraphic column (after Fox and Dolton, 1996) showing reservoirs containing Phosphoria-sourced oil (green circles), with enlargement showing the members of the Phosphoria Formation (after Piper and Link, 2002). Absolute ages of stages are from Gradstein et al. (2004).

Utah, USA (Barbat, 1967; Sheldon, 1967; Stone, 1967). Two members of the Phosphoria Formation, the Meade Peak Phosphatic Shale Member and Retort Phosphatic Shale Member, are organic-rich oil-prone source rocks and are considered to be the main sources of oil in the Phosphoria petroleum system (Claypool et al., 1978; Maughan, 1984). Phosphoria oils in the Bighorn Basin of Wyoming and Montana are produced predominantly from the Pennsylvanian Tensleep Sandstone and Permian Phosphoria Formations, but are also found in Cambrian through Lower Cretaceous units (Fig. 1). The oil is predominantly trapped in structures formed by the Late Cretaceous to Eocene Laramide orogeny.

Permian paleogeographic reconstructions show that the Phosphoria basin was located in eastern Idaho and western Wyoming (Maughan, 1984; Peterson, 1988; Piper and Link, 2002), and developed as a restricted marine basin with upwelling-associated high biological productivity that formed oil-prone source rocks. Along the eastern margin of the basin, porous shelf carbonates developed while farther east impermeable evaporites were deposited in the Goose Egg basin (central and eastern Wyoming).

Oil was generated in the Phosphoria basin in eastern Idaho and western Wyoming as a result of burial by the subsequent deposition of Mesozoic sediments (Claypool et al., 1978; Maughan, 1984), although some oil generation may have been influenced by the development of the Idaho–Wyoming–Utah thrust belt (Edman and Surdam, 1984; Burtner and Nigrini, 1994). The oil migrated eastward along regional dip, was trapped in a regional stratigraphic trap (or series of traps) by the up-dip impermeable evaporites of the Goose Egg Formation, and then re-migrated into structural traps formed by the Laramide orogeny (Campbell, 1956; Cheney and Sheldon, 1959; Campbell, 1962; Sheldon, 1963). Generation and migration occurred prior to the Maastrichtian (Late Cretaceous; ~70 Ma) because the tectonic barriers from the Laramide orogeny later blocked the migration pathways into successor basins such as the Bighorn Basin (Barbat, 1967; Sheldon, 1967; Stone, 1967). Proposed timing of the beginning of oil generation and migration from eastern Idaho and western Wyoming ranges from Late Triassic to Late Cretaceous (Sheldon, 1967; Stone, 1967; Claypool et al., 1978; Edman and Surdam, 1984; Maughan, 1984; Burtner and Nigrini, 1994).

In present-day successor basins such as the Bighorn and Wind River Basins, the Phosphoria Formation consists mainly of porous shelf carbonates which provide excellent reservoir rocks. However, the Meade Peak and Retort Members of the Phosphoria Formation are generally thin, and a limited number of total organic carbon (TOC) analyses of the formation in the Bighorn Basin are reported to be less than 1 wt.% TOC (Claypool et al., 1978; Maughan, 1984). A few Phosphoria core samples from wells along the western margin of the Bighorn Basin (east of Four Bear field, Fig. 1) have TOC values over 3 wt.% and hydrogen index values over 700 mg hydrocarbons/g organic carbon (USGS unpublished data). Some workers have proposed locally derived Phosphoria oils for the Bighorn Basin (Price, 1980; Maughan, 1984; Peterson, 1984; Bjorøy et al., 1996; Stone, 1996; Stone, 2004), and several burial history studies

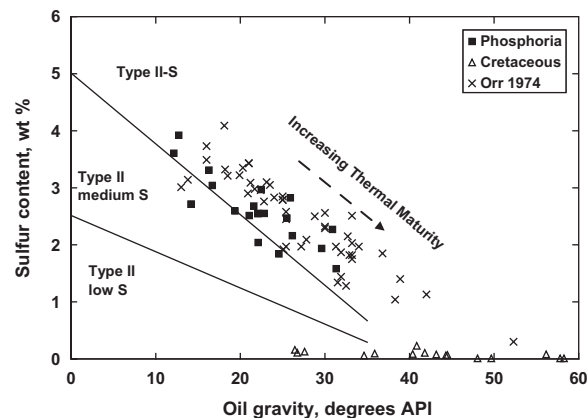


Fig. 2. Sulfur content versus gravity of oils from Bighorn Basin (this study and Orr, 1974) showing Phosphoria-sourced oils in the Type II-S kerogen region (lines from Orr, 2001). Cretaceous-sourced oils in the basin have low sulfur content (data from this study, NIPER, 1995).

have modeled the timing of Phosphoria oil generation in these successor basins. Models in the adjacent Green River and Wind River Basins yielded Late Cretaceous generation ages (Roberts et al., 2004; Kirschbaum et al., 2007; respectively); whereas modeling in the Bighorn Basin yielded Paleocene generation ages (Heasler et al., 1996; Roberts et al., 2008).

The source-rock facies of the Phosphoria Formation has Type II-S kerogen based on kerogen atomic S/C values  $>0.04$  (Lewan, 1985; Sinninghe Damste et al., 1989; Eglinton et al., 1990; Orr and Sinninghe Damste, 1990), and has generated oil with high sulfur content in relation to API gravity (Fig. 2). Some of the Phosphoria oils in the Bighorn Basin have experienced secondary alteration in the reservoir by biodegradation, water washing, thermal cracking, or TSR (Barbat, 1967; Stone, 1967; Orr, 1974; Chung et al., 1981; Clayton, 1991; Bjorøy et al., 1996; Stone, 2004; Roberts et al., 2008).

### 3. METHODS

The crude oil sulfur content was determined using a Carlo Erba 1110 elemental analyzer, and the density of the oils was measured with an Anton Paar DMA 4500 density meter, expressed as American Petroleum Institute (API) gravity in degrees. Crude oil samples were analyzed for  $\delta^{34}\text{S}$  after being filtered with 0.45-micron PTFE syringe filters attached to a Luer-Loc glass syringe. Samples were weighed into tin boats with 1–2 mg of  $\text{V}_2\text{O}_5$  and analyzed for  $\delta^{34}\text{S}$  by continuous flow methods using a Flash 2000 elemental analyzer coupled to a ThermoFinnigan Delta Plus XP mass-spectrometer (Giesemann et al., 1994). Values of  $\delta^{34}\text{S}$  samples are expressed in per mil (‰) relative to the Vienna Canyon Diablo troilite (VCDT) using two nationally accepted standards (NIST standards NBS123 (ZnS) sphalerite with a reported value of  $+17.44 \pm 0.2\text{‰}$  and IAEA-S-3 ( $\text{Ag}_2\text{S}$ ) silver sulfide with a reported value of  $-32.55 \pm 0.12\text{‰}$ ).

Asphaltenes were precipitated from the oils with approximately 40-times volume of iso-octane (for example,

1-g oil to 40-ml solvent) at room temperature. Asphaltene precipitates were separated by centrifugation and filtration with 0.45-micron PTFE syringe filters attached to a Luer-Loc glass syringe. Asphaltenes were dissolved with chloroform and filtered through the aforementioned filter system, dried and weighed.

De-asphalted oils were separated into saturated, aromatic, and polar hydrocarbon fractions using column chromatography with alumina-silica columns and successive elution with iso-octane, benzene, and benzene-methanol azeotrope, respectively. Gas chromatography of whole oil, saturated and aromatic hydrocarbon fractions was performed with an Agilent 6890A gas chromatograph (GC) equipped with a DB-1 capillary column (60-m long by 0.32-mm inner diameter) and a flame ionization detector (FID), using helium as carrier gas at constant flow rate (2.5 ml/min). The inlet and FID temperatures were set at 325 °C. The GC oven temperature was programmed from 40 to 325 °C at 4.5 °C/min with a final hold time of 20 min. The GC was operated in splitless mode, and whole-oils were diluted in carbon disulfide approximately 1:100 w/w prior to injection.

Biological marker distributions of the de-asphalted oil samples were determined on an Agilent 6890 gas chromatograph coupled with a JEOL GCmate magnetic-sector mass spectrometer by selected-ion monitoring (SIM) at mass-to-charge ( $m/z$ ) ratios of 191.1800, 217.1956, 231.1174, and 253.1956. The gas chromatograph used a DB-1 capillary column (60-m long by 0.32-mm inner diameter), splitless injector, and an oven-heating program of 50° to 150 °C at 50 °C/min, 150° to 339 °C at 3 °C/min, and 339 °C for 5 min.

The  $^{13}\text{C}/^{12}\text{C}$  ratios of isolated saturated and aromatic hydrocarbon fractions ( $\text{C}_{15+}$ ) of oil samples were determined using elemental analysis–isotope ratio mass spectrometry (EA–IRMS). Briefly, 0.5 mg of sample is introduced into a Carlo Erba 2500 elemental analyzer via an autosampler. The sample is burned in an oxygen atmosphere at 1030 °C within a chromium oxide-filled quartz reactor. The resulting combustion products are dried over  $\text{MgCl}_2$ ,  $\text{NO}_x$  components reduced to  $\text{N}_2$  over hot copper (600 °C), separated into  $\text{CO}_2$  and  $\text{N}_2$  via isothermal GC (Carbosieve-G, at 0.75 m  $\times$  1/8" @ 70 °C) and introduced into an Finnigan MAT 253 stable isotope ratio mass spectrometer via passive draw open split for subsequent stable carbon isotope analysis.

Carbon isotope values from the instrument undergo off-line isotope corrections for drift and isotopic linearity due to any systematic error introduced in the autosampler, combustion, or chromatographic processes, and are normalized on the Vienna Pee Dee belemnite (VPDB) scale using calibrated, working laboratory standards. The final carbon isotope values represent the average of multiple replicate analyses (generally,  $n > 2$ ) with a standard deviation of generally better than 0.2‰. All final carbon isotope values are reported in delta notation ( $\delta^{13}\text{C}$ , ‰) relative to the VPDB standard.

The Re and Os abundance and isotope compositions of the asphaltene fraction were determined following the protocols outlined in Selby et al. (2007) and Finlay et al. (2010). The asphaltene fraction of the oil was analyzed

because this fraction predominantly hosts >90% of the Re and Os and yields isotope compositions identical to that of a whole-oil analysis (Selby et al., 2007). In brief, 100–200 mg of asphaltene with a known amount of  $^{190}\text{Os}$  and  $^{185}\text{Re}$  tracer solution were placed in a curium tube with 3-ml HCl and 8-ml  $\text{HNO}_3$  and reacted at 220 °C for 48 h. The Os was isolated and purified from the inverse *aqua regia* using  $\text{CHCl}_3$  solvent extraction at room temperature and micro-distillation. The Re was isolated using HCl– $\text{HNO}_3$ -based anion chromatography. The isolated Re and Os were loaded on to Ni and Pt wire filaments, respectively, with the isotope compositions determined by Negative Ionization Mass Spectrometry (NTIMS). The average blanks during the study were  $2.41 \pm 0.05$  pg/g Re and  $0.73 \pm 0.25$  pg/g Os, with an  $^{187}\text{Os}/^{188}\text{Os} = 0.196 \pm 0.006$  ( $n = 3$ ). All data were blank corrected and all uncertainties include the propagated uncertainty in the standard, spike calibrations, mass spectrometry measurements, and blanks. In-house Os (AB-2) and Re (Restd) standard values during this study yield  $^{187}\text{Os}/^{188}\text{Os}$  of  $0.10682 \pm 0.0016$  and  $^{185}\text{Re}/^{187}\text{Re}$  of  $0.59836 \pm 0.00021$  ( $n = 21$ ), respectively. These data are in excellent agreement with previously published studies (Rooney et al., 2010, and references therein). Two samples (14 and 16) were run in replicate through the entire procedure, including separate asphaltene isolation, digestion, and analysis. The  $^{187}\text{Re}/^{188}\text{Os}$  and  $^{187}\text{Os}/^{188}\text{Os}$  data with their  $2\sigma$  uncertainty and associated error correlation Rho were regressed using *Isoplot* (V. 3.72; Ludwig, 2009) using the  $^{187}\text{Re}$  decay constant of  $1.666 \times 10^{-11} \text{ a}^{-1}$  (Smoliar et al., 1996).

#### 4. RESULTS

Oil samples from producing wells (except sample 18—oil from an exploratory well drill-stem test) were selected to be representative of the stratigraphic and geographic distribution of Phosphoria-sourced oils in the Bighorn Basin (Table 1). Elemental and isotopic data from the oils are presented in Table 2. API gravity of the oils ranges from 12.1 to 31.3 degrees, and sulfur content is high ranging from 1.6 to 3.9 wt.%. In contrast, oils derived from Cretaceous sources within the basin (e.g., Mowry and Thermopolis Formations) have sulfur contents less than 0.3 wt.% regardless of oil gravity (Fig. 2). The trend of the Phosphoria oil data in Fig. 2 reflects, in part, a thermal maturity trend in which increasing thermal stress increases the gravity and decreases the sulfur content of oil (Stone, 1967; Orr, 1974; Chung et al., 1981; Bjorøy et al., 1996). However, biodegradation may also influence this trend. The sulfur content-API gravity values (Fig. 2) of the Phosphoria-sourced oils indicate that they are generally derived from type II-S kerogen (Orr, 2001) which is consistent with Phosphoria kerogen analyses (Lewan, 1985; Sinninghe Damste et al., 1989; Eglinton et al., 1990; Orr and Sinninghe Damste, 1990; Price and Wenger, 1992).

The asphaltene fractions of most of the oils are enriched in Re, typically containing tens to hundreds of parts per billion (ppb), with Os abundances of several hundreds to over 4400 parts per trillion (ppt) (Table 2). Three of the 19 samples analyzed are less enriched and contain between one

Table 1  
Sample information of Phosphoria-sourced oils from Bighorn Basin.

Sample	Field name	Well name	Formation	Top (ft)	Lat	Long	Biodegradation <sup>a</sup>	GC comments <sup>b</sup>
1	Butcher Creek	Cruse 1-A	Cloverly (Greybull Mbr. or "Lakota")	260	45.259	-109.533	sats 3/arom 4	Second charge of C <sub>8-17</sub> n-alkanes
2	Cottonwood Creek	Cottonwood Creek Unit 1	Tensleep	5672	44.065	-107.693	sats 0	No arom GC
3	Elk Basin	Unit 193	Bighorn Dolomite	5744	44.970	-108.846	sats 0/arom 2	
4	Elk Basin N.	EBMU 32	Madison	5076	44.999	-108.879	sats 0/arom 0	
5	Fourbear	Unit 31	Tensleep	3325	44.122	-109.258	sats 2/arom 5	Large UCM
6	Frannie	USA PHIL-Rosenburg 27-C	Madison	2925	44.985	-108.636	sats 2/arom 5	Moderate UCM
7	Grass Creek	Unit 10-D	Amsden (Darwin Mbr.)	4480	43.944	-108.659	sats 0/arom 0	Elevated phytane/ $\mu$ C <sub>18</sub>
8	Grass Creek	Stateland 50	Cloverly (Greybull Mbr. or "Lakota")	1993	43.943	-108.660	sats 0/arom 0	Elevated phytane/ $\mu$ C <sub>18</sub>
9	Hamilton Dome	Rathvon 8	Tensleep	2858	43.786	-108.609	sats 0/arom 0	
10	Lamb	Lamb 11	Madison	3752	44.404	-107.979	sats 2/arom 5	Moderate UCM
11	Manderson South	State 2	Tensleep	4255	44.214	-107.801	sats 0/arom 0	High C <sub>30-40</sub> n-alkanes
12	Marshall	USA Texaco 1	Phosphoria	9706	44.123	-107.824	sats 0/arom 0	
13	Rattlesnake	Faure 2A	Phosphoria	10,820	44.079	-107.850	sats 0/arom 0	
14	Torchlight	TLMTU 42	Phosphoria	3178	44.376	-107.987	sats 1/arom 0	Minor UCM
15	Torchlight	TLMTU 50	Madison	3399	44.376	-107.975	sats 1/arom 5	Minor UCM
16	Torchlight	USA Bel C 1	Madison	3818	44.377	-107.992	sats 2/arom 5	Large UCM
17	Torchlight	Orchard Unit 10	Madison and Bighorn Dolomite	3381	44.378	-107.972	sats 1/arom 2	Minor UCM
18	Wildcat	O-Hara Fed. 5-24	Phosphoria	11,071	44.994	-109.254	sats 1/arom 0	Minor UCM
19	Worland	Worland Unit 46 M-F-28	Tensleep	10,172	44.105	-107.901	sats 0/arom 0	

<sup>a</sup> Biodegradation scale of Peters et al. (2005) based on saturated hydrocarbons (sats) and aromatic hydrocarbons (arom).

<sup>b</sup> GC, gas chromatography; UCM, unresolved complex mixture expressed as a baseline hump.

Table 2  
Elemental and isotope data of Phosphoria-sourced oils from Bighorn Basin.

Sample	Gravity <sup>a</sup> °API	S <sup>a</sup> wt. %	Asp <sup>a</sup> wt. %	δ <sup>34</sup> S <sup>a</sup>	δ <sup>13</sup> Csats	δ <sup>13</sup> Carom	CV <sup>b</sup>	Re (ppb)	Os (ppt)	±	<sup>187</sup> Re/ <sup>188</sup> Os	±	<sup>187</sup> Os/ <sup>188</sup> Os	±	rho
1	12.7	3.9	8.4	-6.2	-29.48	-28.58	-0.51	148.1	1038.6	± 0.5	6.7	± 6.1	5.556	± 0.024	0.696
2	21.6	2.7	10.4	-4.6	-29.68	-29.50	-2.05	61.2	729.4	± 0.2	4.4	± 3.6	3.420	± 0.020	0.723
3	24.6	1.8	8.4	-3.4	-28.99	-28.93	-2.53	15.2	313.5	± 0.1	2.7	± 3.4	2.214	± 0.030	0.738
4	29.6	1.9	4.1	-1.2	-28.74	-28.80	-2.87	5.4	130.9	± 0.1	1.6	± 6.5	1.856	± 0.045	0.597
5	12.1	3.6	20.3	-5.4	-29.24	-29.26	-2.63	157.2	1248.2	± 0.5	7.4	± 5.3	4.619	± 0.022	0.705
6	16.3	3.3	9.0	1.7	-28.63	-28.91	-3.40	10.1	272.4	± 0.2	2.5	± 4.3	1.277	± 0.025	0.459
7	22.5	3.0	10.7	-4.7	-29.24	-29.03	-2.12	307.4	4400.1	± 2.4	24.6	± 4.0	3.024	± 0.016	0.294
8	22.8	2.6	7.9	-4.0	-29.40	-28.98	-1.59	89.7	1186.0	± 0.3	6.7	± 2.8	3.082	± 0.017	0.658
9	30.9	2.3	11.4	-4.7	-29.63	-29.36	-1.87	82.8	673.1	± 0.3	4.3	± 5.2	3.414	± 0.022	0.667
10	16.7	3.0	11.3	0.9	-28.13	-28.67	-4.13	142.8	1614.1	± 0.5	5.0	± 2.0	1.963	± 0.005	0.338
11	31.3	1.6	7.2	5.7	-28.28	-28.41	-3.17	3.4	49.1	± 0.1	1.8	± 39.4	3.355	± 0.309	0.853
12	25.9	2.8	3.1	-0.3	-28.94	-28.99	-2.79	81.9	1245.0	± 0.3	6.2	± 2.2	2.293	± 0.012	0.608
13	25.5	2.5	6.1	-1.0	-28.90	-28.92	-2.74	42.0	1196.0	± 0.2	5.7	± 1.2	1.342	± 0.009	0.606
14	22.1	2.5	9.5	4.1	-28.20	-28.52	-3.62	241.3	1381.6	± 0.8	6.4	± 4.8	2.042	± 0.010	0.477
14r								166.4	932.8	± 0.6	4.3	± 5.7	2.053	± 0.010	0.663
15	19.4	2.6	11.8	1.7	-28.33	-28.69	-3.67	96.8	838.5	± 0.3	3.6	± 3.1	1.988	± 0.008	0.480
16	14.2	2.7	15.9	1.9	-28.20	-28.69	-4.00	404.7	1589.1	± 1.3	5.5	± 6.0	2.120	± 0.006	0.436
16r								179.2	760.8	± 0.6	4.1	± 7.8	2.098	± 0.013	0.531
17	21.0	2.5	11.7	-2.8	-29.09	-29.02	-2.48	24.5	515.6	± 0.1	4.7	± 3.5	2.559	± 0.035	0.740
18	22.1	2.0		1.0	-29.22	-28.95	-1.99	0.8	91.3	± 0.0	2.0	± 3.0	0.552	± 0.040	0.472
19	26.2	2.2	8.8	-4.1	-29.27	-29.43	-2.93	72.4	721.1	± 0.2	4.1	± 4.0	3.763	± 0.018	0.720

Re and Os data are from the asphaltene fraction of oil. 14r and 16r are replicate analyses.

<sup>a</sup> Based on whole oil samples. Asp is asphaltene.

<sup>b</sup> CV is canonical variable calculated from δ<sup>13</sup>C of saturated and aromatic hydrocarbons (Sofer, 1984).

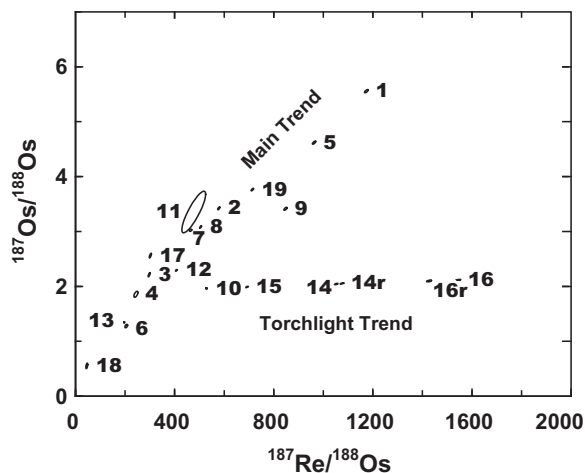


Fig. 3. Re and Os isotope data for the asphaltene fraction of Phosphoria-sourced oils from Bighorn Basin showing two general trends: main trend ( $n = 15$ ) and Torchlight trend ( $n = 4$ ). Data-point ellipses show the 2-sigma error. Data labels are sample numbers listed on Tables 1–3.

and five ppb Re and 49 to 131 ppt Os. Eighteen of the samples possess high  $^{187}\text{Re}/^{188}\text{Os}$  values ( $\sim 196$ – $1546$ ) with radiogenic  $^{187}\text{Os}/^{188}\text{Os}$  values (1.28–5.56). Sample 18 (wildcat) possesses a low  $^{187}\text{Re}/^{188}\text{Os}$  value ( $\sim 45$ ) with only moderately radiogenic  $^{187}\text{Os}/^{188}\text{Os}$  (0.55).

The Re and Os isotope data of the oils show two general trends (Fig. 3). The majority of the oils ( $n = 15$ ) form a steep sloping trend (henceforth called the main trend), which yields a Model 3 Re–Os age of  $239 \pm 43$  Ma with an initial  $^{187}\text{Os}/^{188}\text{Os}$  value of  $0.85 \pm 0.42$  and a mean square weighted deviation (MSWD) of 1596 (Fig. 4). Outliers on this trend are oils from Hamilton Dome (sample 9) and Manderson South (sample 11) fields, with the latter sample having a significant error ellipse. The second trend in the Re–Os data is shown by four oils from the Torchlight (samples 14–16) and Lamb (sample 10) fields (henceforth called the Torchlight trend). These oils are also considered to be derived from the Phosphoria Formation (Orr, 1974; Bjorøy et al., 1996). However, the Re–Os data yield a Model 1 isochron of Miocene age ( $9.24 \pm 0.39$  Ma) with an initial  $^{187}\text{Os}/^{188}\text{Os}$  value of  $1.88 \pm 0.01$  and a MSWD of 0.05 (Fig. 5). An isochron that includes two replicate analyses (samples 14r and 16r, Table 2) is nearly identical ( $9.24 \pm 0.38$  Ma, initial  $^{187}\text{Os}/^{188}\text{Os} = 1.88 \pm 0.01$ ; MSWD = 0.49, Model 1,  $n = 6$ ).

The  $\delta^{34}\text{S}$  values of the oils range from  $-6.2\text{‰}$  to  $+5.7\text{‰}$  (VCDT), similar to Phosphoria-sourced oils of previous studies (Thode et al., 1958; Vredenburg and Cheney, 1971; Orr, 1974). The vast majority of Phosphoria-sourced oils from the Bighorn and Wind River Basins range in value from  $-7\text{‰}$  to  $-2\text{‰}$ , whereas oils with heavier isotopic values may have been altered by TSR (Orr, 1974). The distribution of  $\delta^{34}\text{S}$  values in this study is similar in that a natural break exists at about  $-2\text{‰}$  dividing the oils into two groups (Fig. 6). We will assume that  $\delta^{34}\text{S}$  values of the oils greater than  $-2\text{‰}$  are a proxy for TSR. On this basis, two groups can be designated—non-TSR and TSR—with the Torch-

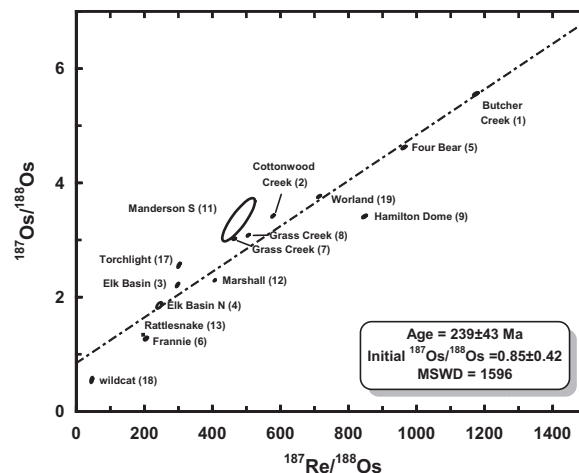


Fig. 4. Re–Os isotope data of Phosphoria-sourced oils from the main trend (Fig. 3), Bighorn Basin, showing the calculated regression age. Data-point ellipses show the 2-sigma error. Data labels are field names and sample numbers listed on Table 1.

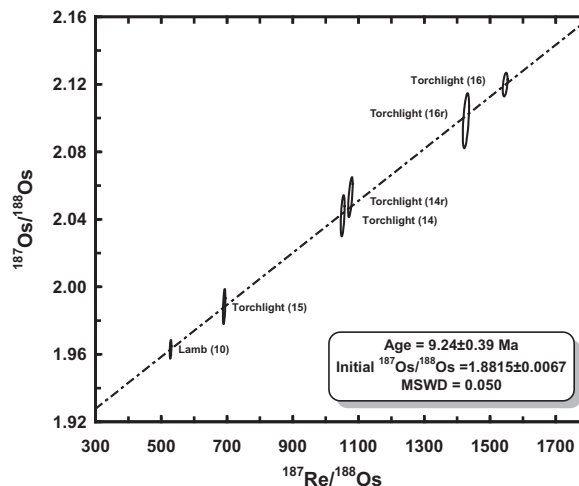


Fig. 5. Re–Os isochron of Phosphoria-sourced oils from the Torchlight trend (Torchlight and Lamb fields), Bighorn Basin. Data-point ellipses show the 2-sigma error. Data labels are field names and sample numbers listed on Table 1.

light trend oils falling in the range of the TSR group (Fig. 6). The non-TSR oils show a weak inverse trend in relation to sulfur content whereas the TSR and Torchlight trend oils show no obvious trend.

The ranges of  $\delta^{13}\text{C}$  values for the saturated and aromatic hydrocarbon fractions are  $-29.68\text{‰}$  to  $-28.13\text{‰}$  and  $-29.50\text{‰}$  to  $-28.41\text{‰}$  (VPDB), respectively, and are similar to Phosphoria-sourced oils from the Bighorn Basin reported in previous studies (Chung et al., 1981; Silliman et al., 2002; Lillis et al., 2003). On Fig. 7 the Phosphoria oils plot in the nonwaxy (marine) oil region as defined by Sofer (1984), although Butcher Creek (sample 1) plots closer to the waxy (terrigenous) oil region of the figure. The TSR and Torchlight trend oils are isotopically heavier, especially the saturated hydrocarbon fraction, consistent with oils al-

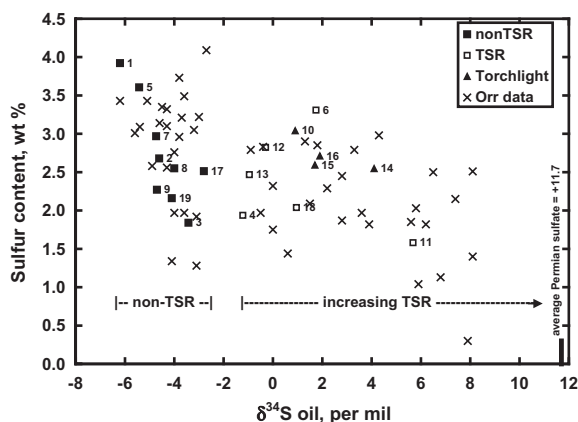


Fig. 6. Sulfur content as a function of  $\delta^{34}\text{S}$  values of Phosphoria-sourced oils from Bighorn Basin (this study and Orr, 1974) showing the effects of thermochemical sulfate reduction (TSR). Oils are divided into non-TSR or TSR (includes Torchlight trend oils) at the natural break at  $-2\text{‰}$ . Average Permian sulfate is from Ault and Kulp (1959) and Vredenburg and Cheney (1971).

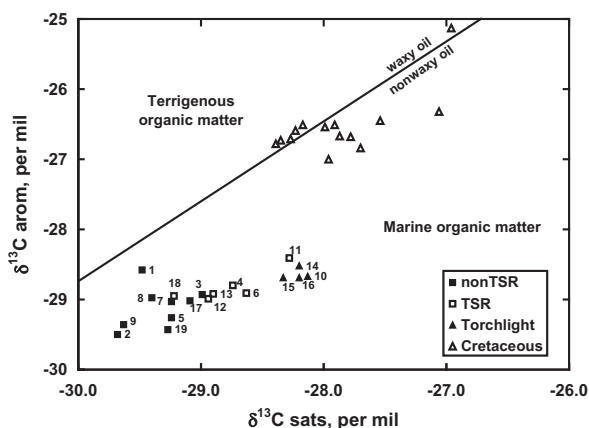


Fig. 7. Stable carbon isotope ratios ( $\delta^{13}\text{C}$ ) of aromatic and saturated hydrocarbon fractions for oils from Bighorn Basin. The diagonal line separates waxy oil (derived from terrigenous organic matter) from nonwaxy oil (derived from marine organic matter) (Sofer, 1984).

tered by TSR (Claypool and Mancini, 1989; Manzano et al., 1997). Oils derived from Cretaceous source rocks in the Bighorn Basin are isotopically heavier than Phosphoria-sourced oils (Fig. 7).

Gas chromatograms of whole oils, as well as those of saturated and aromatic hydrocarbon fractions, provide genetic and secondary petroleum alteration information. Pristane/phytane values range from 0.5 to 0.8 except Butcher Creek (sample 1), which has a value of 1.1 (Table 3). The pristane/phytane values (less than unity) are consistent with measurements of Phosphoria oils in other studies (Stone, 1996; Silliman et al., 2002; Lillis et al., 2003; Kirschbaum et al., 2007), and similar to bitumen extracts of the Phosphoria Formation (Claypool et al., 1978; Price and Wenger, 1992; Dahl et al., 1993). Pristane/ $n\text{-C}_{17}$  and phytane/ $n\text{-C}_{18}$

values range from 0.26 to 1.11 and 0.36 to 2.01, respectively. These values correlate with the Phosphoria-sourced oils of Silliman et al. (2002), except that oil samples 1, 5, 6, 10, and 16 have elevated values due to biodegradation. These parameters do not appear to discriminate TSR oils from non-TSR oils, whereas pristane/ $n\text{-C}_{17}$  and phytane/ $n\text{-C}_{18}$  values decrease and pristane/phytane values increase in oils exposed to laboratory-simulated TSR experiments (Zhang et al., 2008).

The effects of biodegradation are reflected in the gas chromatograms (e.g., Fig. 8) and were rated using a zero to ten scale (Peters et al., 2005; Fig. 16.11). Most of the oils are nonbiodegraded (level 0), and none of the oils are biodegraded beyond level 3 based on the saturated hydrocarbons ( $n$ -alkanes completely eliminated and acyclic isoprenoids substantially depleted) and level 5 based on aromatic hydrocarbons (methyl-, dimethyl-, trimethylnaphthalenes and methylphenanthrenes eliminated) (Table 1). In some cases oils rate a higher level of biodegradation based on aromatic hydrocarbons than based on saturated hydrocarbons (for example, samples 1, 3, 5, 6, 10, 15, 16, and 17). Biodegradation and water washing effects on crude oil in a reservoir are sometimes difficult to distinguish as the two processes often occur together, and their effects on crude oil are similar in some respects. One distinguishing characteristic of water washing is the preferential removal of light aromatic hydrocarbons due to their higher solubility in water relative to  $n$ -alkanes of the same carbon number (Palmer, 1984; Lafargue and Barker, 1988; Kuo, 1994). Oils showing higher values on the biodegradation scale based on aromatic hydrocarbons relative to saturated hydrocarbons may be reflecting the effects of water washing (Table 1). Bjorøy et al. (1996) observed a number of Phosphoria-sourced oils in the Bighorn Basin with a greater degree of water washing than biodegradation.

Biomarker data (Table 3) of the oils provide genetic, thermal maturity, and secondary petroleum alteration information. Biomarkers that reflect genetic (gammacerane/hopane,  $C_{35}/C_{31}\text{--}C_{35}$  homohopanes) and mixed genetic and maturity information ( $T_s/T_s + T_m$ ,  $C_{23}$  tricyclic/ $C_{23}$  tricyclic +  $C_{30}$  hopane) of the oils are similar to the bitumen extracts of the Meade Peak and Retort Members of the Phosphoria Formation (Dahl et al., 1993). Biomarkers that reflect the thermal maturity of the oils ( $(C_{20} + C_{21})/(C_{20} + C_{21} + C_{26} + C_{27} + C_{28})$  triaromatic steroids, TAS) are also comparable to that of the Phosphoria bitumen extracts of Dahl et al. (1993) except samples 11 and 18 show a higher level of thermal maturity based on the triaromatic steroids (TAS) ratio (Table 3). Bjorøy et al. (1996) utilized the TAS ratio to evaluate the thermal maturity of Phosphoria-sourced oils in the Bighorn Basin and found that most oils were of “normal” maturity with TAS values less than 0.3, comparable to values in this study (Table 3). Based on the hydrous pyrolysis experiments of Lewan et al. (1986), the TAS value of 0.3 marks the end of bitumen generation and the beginning of oil generation from the Retort Phosphatic Shale Member of the Phosphoria Formation. Biomarkers can be altered by biodegradation at more severe levels (Peters et al., 2005). However, none of the oils in this study have been biodegraded to a level that affects

Table 3

Biomarker data of Phosphoria-sourced oils from Bighorn Basin and source rocks of the Phosphoria Formation.

Sample	Pr/Ph <sup>a</sup>	Pr/17 <sup>a</sup>	Ph/18 <sup>a</sup>	C <sub>26</sub> /T <sup>b</sup>	Ts/Tm <sup>c</sup>	C <sub>23</sub> /H <sup>d</sup>	Gam/H <sup>e</sup>	C <sub>35</sub> /HH <sup>f</sup>	Diast <sup>g</sup>	TAS <sup>h</sup>	C29SR <sup>i</sup>	C29β <sup>j</sup>
<i>Oils</i>												
1	1.13	1.11	2.01	2.33	0.25	0.47	0.21	0.14	0.25	0.10	0.43	0.57
2	0.60	0.26	0.46	2.06	0.24	0.60	0.20	0.15	0.18	0.15	0.47	0.62
3	0.64	0.28	0.48	2.01	0.29	0.63	0.21	0.15	0.26	0.19	0.44	0.57
4	0.66	0.26	0.42	2.00	0.31	0.66	0.21	0.15	0.29	0.18	0.43	0.57
5	0.68	0.69	1.14	1.88	0.29	0.49	0.20	0.14	0.24	0.09	0.45	0.58
6	0.61	0.69	1.31	1.97	0.21	0.60	0.18	0.14	0.25	0.15	0.41	0.60
7	0.49	0.40	0.95	1.81	0.24	0.45	0.30	0.18	0.52	0.08	0.45	0.57
8	0.56	0.44	0.88	1.67	0.25	0.61	0.22	0.19	0.73	0.09	0.48	0.60
9	0.57	0.27	0.48	2.03	0.25	0.54	0.21	0.13	0.23	0.15	0.42	0.59
10	0.57	0.66	1.13	1.69	0.29	0.67	0.21	0.17	0.17	0.16	0.42	0.51
11	0.63	0.31	0.48	1.66	0.32	0.71	0.17	0.18	0.23	0.46	0.39	0.49
12	0.49	0.35	0.71	2.30	0.24	0.56	0.19	0.15	0.18	0.13	0.46	0.60
13	0.57	0.32	0.58	1.94	0.24	0.57	0.23	0.15	0.25	0.17	0.47	0.61
14	0.54	0.47	0.91	1.50	0.28	0.69	0.18	0.13	0.22	0.20	0.46	0.59
15	0.62	0.51	0.80	1.56	0.27	0.69	0.17	0.13	0.23	0.16	0.48	0.61
16	0.52	1.01	1.98	1.61	0.28	0.69	0.20	0.13	0.23	0.17	0.47	0.60
17	0.59	0.38	0.69	1.90	0.27	0.61	0.19	0.14	0.22	0.22	0.45	0.57
18	0.69	0.33	0.52	1.88	0.30	0.71	0.21	0.14	0.18	0.33	0.51	0.57
19	0.80	0.26	0.36	2.31	0.28	0.59	0.18	0.16	0.21	0.22	0.43	0.54
<i>Rocks</i>												
Retort (3) <sup>k</sup>	0.81				0.34	0.23	0.20	0.20		0.09		
Meade (7) <sup>k</sup>	0.51				0.21	0.57	0.13	0.12		0.12		

<sup>a</sup> Pristane/Phytane, 17 = *n*-C<sub>17</sub>, 18 = *n*-C<sub>18</sub>, values from whole-oil gas chromatograms.<sup>b</sup> C<sub>26</sub> (R + S) tricyclic terpanes/C<sub>24</sub> tetracyclic terpene.<sup>c</sup> 18α-22,29,30-trisnorneohopane/(17α-22,29,30-trisnorhopane + 18α-22,29,30-trisnorneohopane).<sup>d</sup> C<sub>23</sub> tricyclic terpene/[C<sub>30</sub> 17α,21β(H) hopane + C<sub>23</sub> tricyclic terpene].<sup>e</sup> Gammacerane/C<sub>30</sub> 17α,21β(H) hopane.<sup>f</sup> [C<sub>35</sub> 17α,21β(H) 22S + 22R hopanes]/[C<sub>31</sub>–C<sub>35</sub> 17α,21β(H) 22S + 22R hopanes].<sup>g</sup> C<sub>27</sub> 13β,17α(H)-20S diacholestane/C<sub>27</sub> 5α,14α,17α(H) 20R cholestane.<sup>h</sup> (C<sub>20</sub> + C<sub>21</sub>)/(C<sub>20</sub> + C<sub>21</sub> + C<sub>26</sub> + C<sub>27</sub> + C<sub>28</sub>) triaromatic steroids.<sup>i</sup> 20S/(20S + 20R) 5α,14α,17α(H) 24-ethylcholestane.<sup>j</sup> 5α,14β,17β (H)/[5α,14α,17α (H) + 5α,14β,17β (H)] 20R 24-ethylcholestane.<sup>k</sup> Retort and Meade (*n* = number of samples) are average values from bitumen extracts of the Retort and Meade Peak Members of the Phosphoria Formation (Dahl et al., 1993).

the biomarkers analyzed (*m/z* 191.1800, 217.1956, 231.1174, and 253.1956 mass chromatograms).

## 5. DISCUSSION

### 5.1. Re–Os geochronometry of the main-trend oils

The Re–Os isotope data on Fig. 3 show two different age trends. The main trend (Fig. 4) involving 15 of the 19 oils yields a Model 3 Re–Os age of 239 ± 43 Ma (initial <sup>187</sup>Os/<sup>188</sup>Os = 0.85 ± 0.42; MSWD = 1596). This Middle Triassic Re–Os age is younger than that of the source rock (Permian) and older than the proposed timing of oil generation and migration (Late Triassic to Late Cretaceous; Sheldon, 1967; Stone, 1967; Claypool et al., 1978; Edman and Surdam, 1984; Maughan, 1984; Burtner and Nigrini, 1994). However, there is considerable age uncertainty (±43 Ma) and significant scatter about the regression (MSWD = 1596). For isotopic data to yield a linear array, all samples must possess the same initial <sup>187</sup>Os/<sup>188</sup>Os values, have formed at the same time, and not be affected by any post-formation geochemical alteration. Possible reasons

for the observed scatter in the main-trend regression include variations in the initial <sup>187</sup>Os/<sup>188</sup>Os values of the Phosphoria Formation, duration of petroleum generation, the process of oil migration, and petroleum alteration in the reservoir by thermochemical sulfate reduction (TSR).

#### 5.1.1. Initial <sup>187</sup>Os/<sup>188</sup>Os values of the source rock

The initial <sup>187</sup>Os/<sup>188</sup>Os value of a source rock reflects local seawater at the time of deposition (Ravizza and Turekian, 1989). The initial <sup>187</sup>Os/<sup>188</sup>Os value of crude oil at the time of generation is interpreted as a function, in part, of the initial <sup>187</sup>Os/<sup>188</sup>Os value of its source rock and the radiogenic in-growth since deposition (Selby et al., 2007; Finlay et al., 2011). With the exception of the oil from Butcher Creek field (sample 1), the source of the oils in this study is interpreted to be the Phosphoria Formation. The Butcher Creek oil is a biodegraded Phosphoria-sourced oil that has a second charge of high-gravity Cretaceous(?) oil, based on the appearance of the gas chromatograms (Fig. 8), pristane/phytane value >1, lower than expected asphaltene content (Table 2), and a slightly higher δ<sup>13</sup>C aromatic hydrocarbon value (Fig. 7). However, this oil aligns

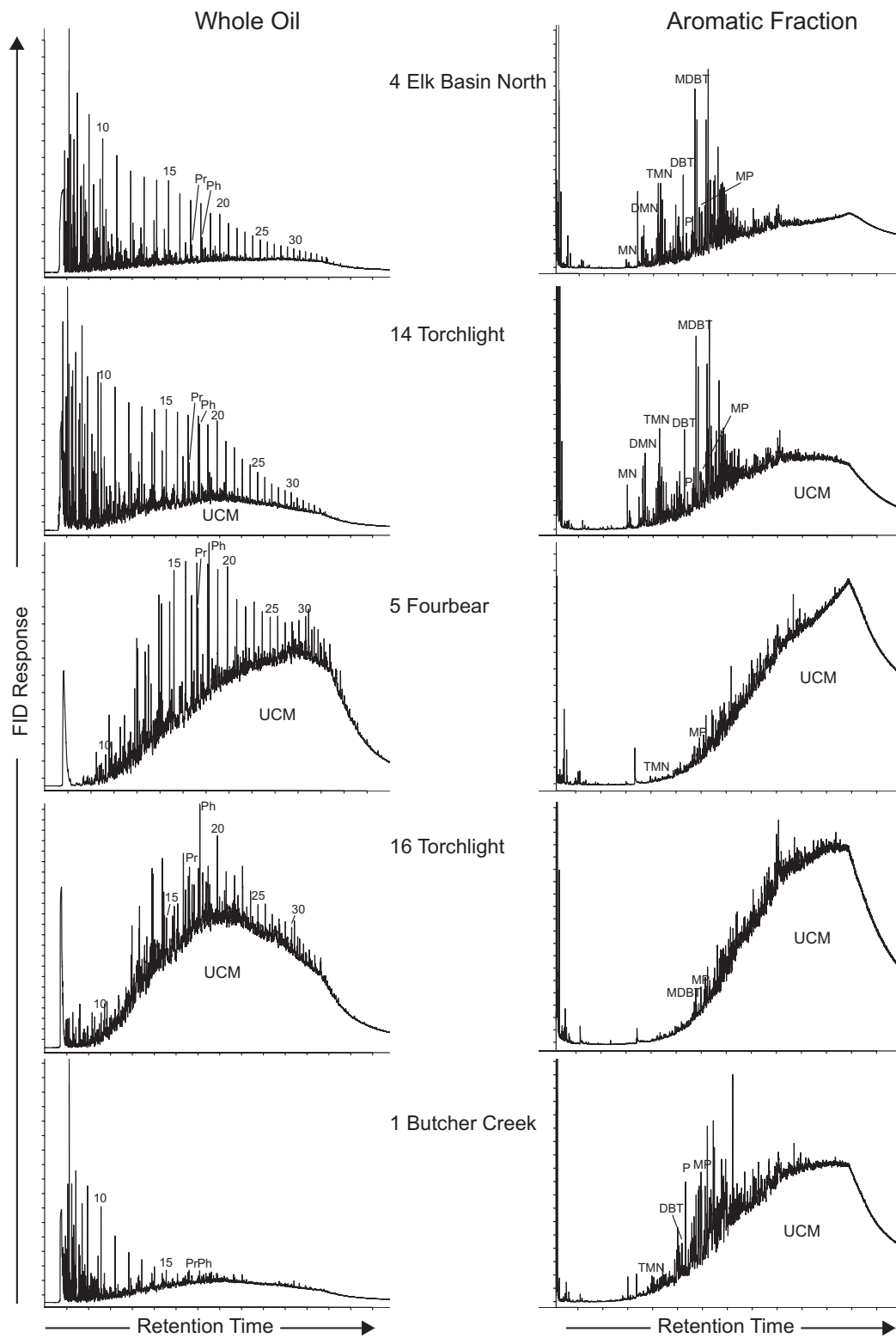


Fig. 8. Selected gas chromatograms of whole oil and aromatic hydrocarbon fractions, showing increasing biodegradation and water washing (top to bottom). Butcher Creek field has a second charge of light oil. Numbers are *n*-alkane carbon numbers. Pr, pristane; Ph, phytane; MN, methylnaphthalenes; DMN, dimethylnaphthalenes; TMN, trimethylnaphthalenes; DBT, dibenzothiophene; P, phenanthrene; MDBT, methyl dibenzothiophenes; MP, methylphenanthrenes; UCM, unresolved complex mixture.

well with the main trend (Fig. 4) suggesting that the second charge contains little or no asphaltenes and thus would not contribute much Re or Os to the original oil.

The two Phosphoria source members, Meade Peak and Retort, span over 5 m.y. of marine deposition (Fig. 1) and contain discernable differences in geochemical composition reflecting their depositional environments (Dahl et al., 1993). Previous studies have identified subtypes of Phosphoria-sourced oils, but have not correlated these subtypes to a specific member of the Phosphoria Formation (Bjørøy et al., 1996; Silliman et al., 2002). Similarly, the genetic biomarker parameters of oils in this study (Table 3) are generally intermediate in composition between the Meade Peak and Retort bitumen extracts of Dahl et al. (1993), suggesting that both members are sources of these oils. However, samples 7 and 8 from Grass Creek field appear to correlate better with the Retort Phosphatic Shale Member based on  $C_{35}/C_{31}-C_{35}$  homohopane values. Sample 7 also has anomalously high Re and Os content. Based on the available data, the oils in the main trend, with the possible exception of Grass Creek, are interpreted to be derived from both members of the Phosphoria Formation.

The range of  $^{187}\text{Os}/^{188}\text{Os}$  values within the Phosphoria Formation is unknown. The temporal resolution of the marine Os isotope record through the Phanerozoic is poor due to a paucity of data, but significant variations during short (<1 m.y.) time intervals have been documented (Cohen et al., 1999; Peucker-Ehrenbrink and Ravizza, 2000; Turgeon and Creaser, 2008; Georgiev et al., 2011). Thus, part of the scatter in the main-trend regression may reflect variations in the initial  $^{187}\text{Os}/^{188}\text{Os}$  values due to the evolution of sea water chemistry over 5 m.y. from the beginning of Meade Peak to the end of Retort Member deposition.

#### 5.1.2. Duration of petroleum generation

Previous studies have suggested that the age derived from a Re–Os isochron of petroleum reflects the timing of oil generation or migration (Selby et al., 2005; Selby and Creaser, 2005b; Finlay et al., 2011). However, petroleum generation is not an instantaneous event, but may span millions of years depending on the burial and thermal history of the source rock and the generation kinetics of the source kerogen. For example, one-dimensional (1-D) burial-history models for wells in the Greater Green River Basin in southwestern Wyoming using Phosphoria Type II-S kinetics (Lewan, 1985) showed the duration of Phosphoria oil generation to range from 8 to 15 m.y (Roberts et al., 2004). The generative area (so-called petroleum source kitchen) of the Phosphoria petroleum system covers a four-state area including Montana, Idaho, Wyoming, and Utah, with the Meade Peak Phosphatic Shale Member occupying an area of approximately 118,000 km<sup>2</sup> and the Retort Phosphatic Shale Member occupying 143,000 km<sup>2</sup> (Maughan, 1975). Oil generation progressed from west to east starting as early as Late Triassic in eastern Idaho with the oil window moving to western Wyoming by Early Cretaceous (Stone, 1967; Maughan, 1984; Stone, 2004). A two-dimensional burial-history model for eastern Idaho-western Wyoming constructed by Burtner and Nigrini (1994) shows the Phosphoria oil window moving eastward through time

from 160 to 88 Ma during the development of the Idaho-Wyoming thrust belt, indicating that the duration of Phosphoria oil generation from the source kitchen may have been over 70 million years. Oil trapped in a field represents the cumulative charge throughout the duration of oil generation if migration paths remain intact in the same time frame (Larter and Aplin, 1995). Thus, even if one assumes that the oil fields in the Bighorn Basin were directly charged from the source kitchen, the duration (>70 m.y.) of the Phosphoria oil window would cause scatter and imprecision in the main-trend regression.

#### 5.1.3. Effects of oil migration

Oil migration of the Phosphoria petroleum system is widely regarded as a two-step process. Oil was generated from the Phosphoria Formation in eastern Idaho and western Wyoming, migrated eastward to central Wyoming where it was sequestered in a regional stratigraphic trap (or series of traps) until the Laramide orogeny formed the Bighorn Basin and structural traps that the oil resides in today. It is unclear whether oil migration affects Re–Os isotope systematics. The process of oil migration may homogenize the oil to some degree and possibly reset the Re–Os isotope isochron, but it cannot account for the range in Re/Os values observed in a set of oils from a single petroleum system (Selby and Creaser, 2005b). The main-trend regression age (Triassic) does not appear to reflect the timing of re-migration (Late Cretaceous to Eocene) although the process may contribute to the scatter in the regression. It is likely that the migration and charging history of the Bighorn Basin oil fields is much more complicated, and each field has a distinct filling history. In future studies, isochrons constructed from oil samples from an individual field will likely yield a more precise result (e.g., Torchlight oils, see Section 5.2).

#### 5.1.4. Effects of biodegradation and water washing

Biodegradation has been discounted as a significant effect on Re–Os isotope systematics (Selby et al., 2005; Selby and Creaser, 2005b; Finlay et al., 2011) based on the observation that most Re and Os in crude oil reside in the asphaltene fraction, which is more resistant to biodegradation, and that Re–Os isochrons from degraded oils have yielded low MSWD values. Similarly, the effects of water washing are unlikely to alter the Re and Os values because the asphaltene fraction has a much lower aqueous solubility than the saturated and aromatic hydrocarbon fractions in crude oil. To test these alteration effects, a regression of Re–Os isotope data was calculated from oils in the main trend that excluded the three most degraded oils from biodegradation or water washing. Excluding Butcher Creek (sample 1), Fourbear (sample 5) and Frannie (sample 6), the calculated regression yields a Model 3 Re–Os age of  $232 \pm 77$  Ma (initial  $^{187}\text{Os}/^{188}\text{Os} = 0.93 \pm 0.61$ ; MSWD = 1990,  $n = 12$ ). Clearly, this does not reduce the scatter (MSWD is higher). Furthermore, visual inspection of Fig. 4 shows that Butcher Creek and Four Bear oils align on the main trend more closely than the nondegraded outlier oils from Hamilton Dome (sample 9) and Manderson South (sample 11). Finally the Torchlight trend oils

(Fig. 5) are all slightly biodegraded (level 1–2) and most are water washed (aromatics at level 5), yet the isochron has very little scatter (MSWD of less than one). Thus biodegradation and water washing (at this level of alteration) do not appear to be significant causes of scatter in the regression of the main trend (Fig. 4).

#### 5.1.5. Effects of thermal cracking in the reservoir

Thermal maturity of crude oil is a function of its generation and reservoir thermal history (Tissot and Welte, 1984, p. 461; Clayton, 1991). Previous studies have proposed that some of the Phosphoria-sourced oils from the Bighorn Basin have experienced thermal cracking in the reservoir (Barbat, 1967; Stone, 1967; Orr, 1974; Chung et al., 1981; Clayton, 1991; Bjorøy et al., 1996; Heasler et al., 1996; Roberts et al., 2008). However, Price (1997) concluded that no in-reservoir thermal cracking has occurred in the Phosphoria-sourced oils studied by Orr (1974) because reservoir temperatures are too low (80–120 °C). Bjorøy et al. (1996) utilized the TAS ratio to evaluate the thermal maturity of Phosphoria-sourced oils in the Bighorn Basin and found that most oils were of “normal” maturity with TAS values less than 0.3, comparable to values of most of the oils in this study (Table 3). Roberts et al. (2008) modeled Phosphoria oil cracking in wells in deeper portions of the basin using the cracking kinetics of Tsuzuki et al. (1999) and concluded that Phosphoria oil cracking only occurred in three of the deepest wells (present-day depths greater than 20,000 feet with another 4500–6500 feet of overburden removed). However, oils in this study and most oil production in the basin come from reservoirs at present-day depths less than 11,000 feet (Table 1) and are unlikely to have experienced the necessary thermal history for in-reservoir cracking.

Oils in this study show minor variations in stable carbon isotopes, gravity, sulfur content, pristane/*n*-C<sub>17</sub>, phytane/*n*-C<sub>18</sub> and biomarker maturity parameters that may reflect, in part, variations in biodegradation, water washing, TSR, and thermal maturity from oil generation. In contrast, evidence for significant in-reservoir thermal cracking is not apparent. Increases in  $\delta^{13}\text{C}$  values previously attributed to in-reservoir cracking (Orr, 1974; Chung et al., 1981; Clayton, 1991) may be caused by oxidation during TSR (Fig. 9a and b). There are, however, examples of oils in other studies in the Bighorn Basin that appear to have been thermally cracked in the reservoir, e.g., 52 API gravity oil at Fivemile field (Orr, 1974) and 42 API gravity oil at Golden Eagle field (Bjorøy et al., 1996).

A possible exception in this study is the oil from Manderson South (sample 11) which has the highest thermal maturity based on the TAS ratio and API gravity. It also has the lowest osmium and sulfur content, and the largest error ellipse in Re–Os isotope data (Fig. 4). This oil has possibly re-migrated from deeper in the basin (Orr, 1974) and may have experienced some thermal cracking. Alternatively, this oil has a high TAS value due to thermochemical sulfate reduction (Bjorøy et al., 1996), which is supported by its high  $\delta^{34}\text{S}$  value (Table 2). Thus, with the possible exception of Manderson South, thermal cracking in the reservoir does not appear to be a significant cause of scatter in the Re–Os regression of the main trend (Fig. 4). However,

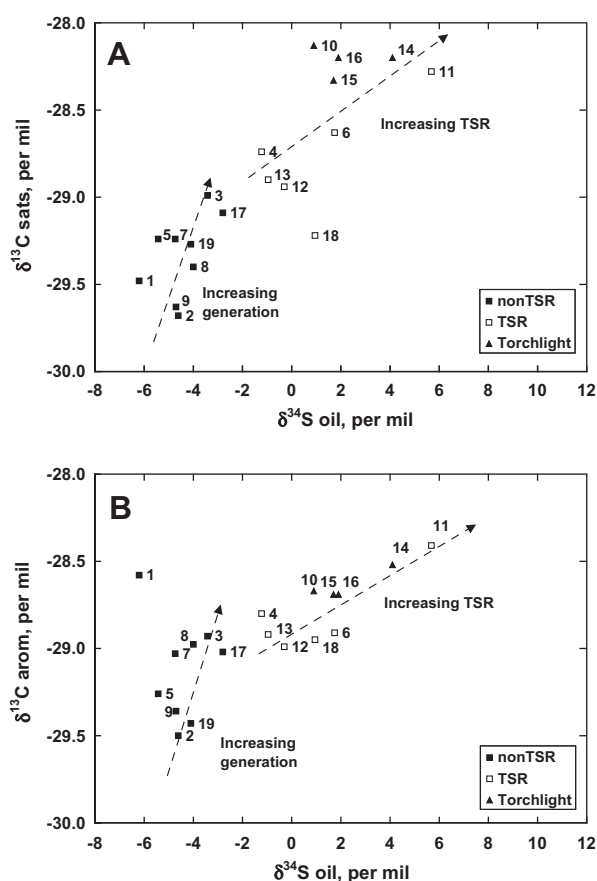


Fig. 9. Plots of (a)  $\delta^{13}\text{C}$  saturated hydrocarbons or (b)  $\delta^{13}\text{C}$  aromatic hydrocarbons as a function of  $\delta^{34}\text{S}$  of Phosphoria-sourced oils from Bighorn Basin showing the effects of increasing thermochemical sulfate reduction and thermal maturity from oil generation.

the results presented here do not preclude the possibility that thermal cracking may disrupt Re–Os isotope systematics in other cases.

#### 5.1.6. Effects of thermochemical sulfate reduction

Thermochemical sulfate reduction (TSR) is a post-accumulation alteration process that occurs in reservoirs containing anhydrite ( $\text{CaSO}_4$ ) or another source of sulfate where petroleum is oxidized to  $\text{CO}_2$  and sulfate is reduced to sulfide (Goldstein and Aizenshtat, 1994; Machel et al., 1995). Other primary and secondary products of TSR include solid bitumen, metal sulfides, carbonate minerals, water, and various organosulfur compounds within the oil. Minimum onset temperatures are between 100 and 140 °C (Machel, 2001) although Orr (1974) suggested TSR can occur at temperatures as low as 80 °C in his pioneering study of TSR in the Bighorn Basin. Recent research suggests that there is a range of minimum temperatures depending on the petroleum composition, reservoir conditions, initial  $\text{H}_2\text{S}$  content, kinetics of the reaction, and availability of anhydrite (Machel, 2001; Zhang et al., 2007). An important geochemical change in petroleum altered by TSR

is that the  $\delta^{34}\text{S}$  of the oil approaches the value of the reacting sulfate mineral.

Orr (1974) showed that the  $\delta^{34}\text{S}$  values of some of the Phosphoria oils in the Bighorn Basin are isotopically heavier as a result of TSR utilizing the isotopically heavy sulfate (anhydrite) in the Phosphoria and equivalent evaporate formations (Goose Egg Formation). He suggested that unaltered Phosphoria oils have  $\delta^{34}\text{S}$  values averaging about  $-4\text{‰}$  and oils altered by TSR have  $\delta^{34}\text{S}$  values as high as  $+8\text{‰}$  approaching the composition of Permian sulfate (average  $+11.7\text{‰}$ , Ault and Kulp 1959; Vredenburg and Cheney, 1971; Fig. 6). Because the lithofacies transition between the Phosphoria Formation (carbonates) and Goose Egg Formation (evaporites) lies along the eastern edge of the Bighorn Basin (Campbell, 1962), most of the TSR-altered oils (as reflected by high  $\delta^{34}\text{S}$  values) reside in fields along the east side where higher concentrations of sulfate are available. Our  $\delta^{34}\text{S}$  results are similar to the results of Orr (1974) and correspond spatially in that the highest  $\delta^{34}\text{S}$  values lie along the eastern edge of the basin (Fig. 10). The distribution of values of all data from the basin (this study and Orr, 1974) has a mode of  $-4.3\text{‰}$  and a natural break between  $-2.7\text{‰}$  and  $-1.2\text{‰}$  (Fig. 6). The distribution of  $\delta^{34}\text{S}$  values of Phosphoria-sourced oils in the Wind River Basin (mode =  $-5.4\text{‰}$ , Vredenburg and Che-

ney, 1971) is very similar to that in the Bighorn Basin except that there are very few oils in the Wind River Basin altered by TSR. We interpret the modal groups in both basins to be Phosphoria-sourced oils without TSR alteration, and oils with  $\delta^{34}\text{S}$  greater than  $-2\text{‰}$  to have increasing amounts of TSR alteration. Based on this  $\delta^{34}\text{S}$  proxy, the Manderson South (sample 11) oil is the most altered by TSR. The Torchlight trend oils also have isotopically high  $\delta^{34}\text{S}$  values ( $+0.9\text{‰}$  to  $+4.1\text{‰}$ ) consistent with TSR alteration (Fig. 6). One oil from Torchlight field (sample 17) falls in the main trend (Fig. 4) and is apparently not altered by TSR based on its low  $\delta^{34}\text{S}$  value ( $-2.8\text{‰}$ ). Bjorøy et al. (1996) analyzed the same oil (their sample W4-20) and interpreted it to be normal maturity oil not altered by TSR based on low dibenzothiophene and TAS ratios. We concur that this oil is not altered by TSR because it resides in an older reservoir (Ordovician Bighorn Dolomite and Mississippian Madison Limestone) where the oil is not in contact with sulfate minerals (or concentrated dissolved sulfate) as is the case in Torchlight field oils in younger reservoirs (samples 14–16).

Plots of  $\delta^{34}\text{S}$  and  $^{187}\text{Re}/^{188}\text{Os}$  (Fig. 11a) and  $^{187}\text{Os}/^{188}\text{Os}$  (Fig. 11b) show inverse linear trends for the non-TSR oils, and no trend for the TSR oils, strongly suggesting that TSR disrupts Re–Os isotope systematics. The cause of the in-

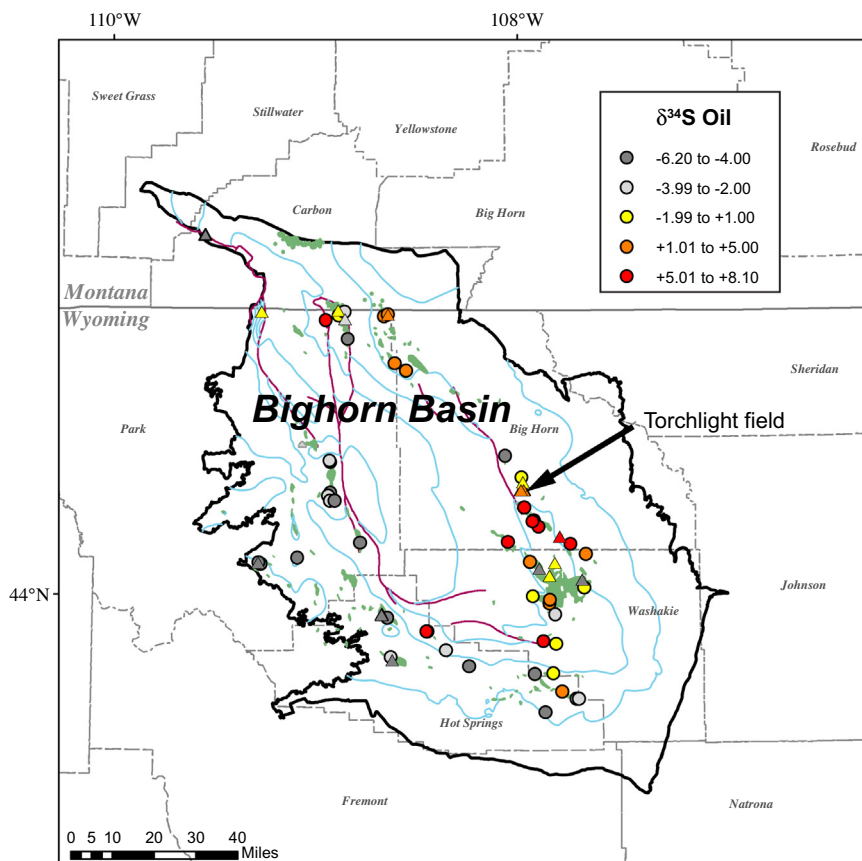


Fig. 10. Map of  $\delta^{34}\text{S}$  values of Phosphoria-sourced oils from Bighorn Basin showing the highest values along the eastern margin of the basin caused by thermochemical sulfate reduction. Circles are data from Orr (1974) and triangles are data from this study.

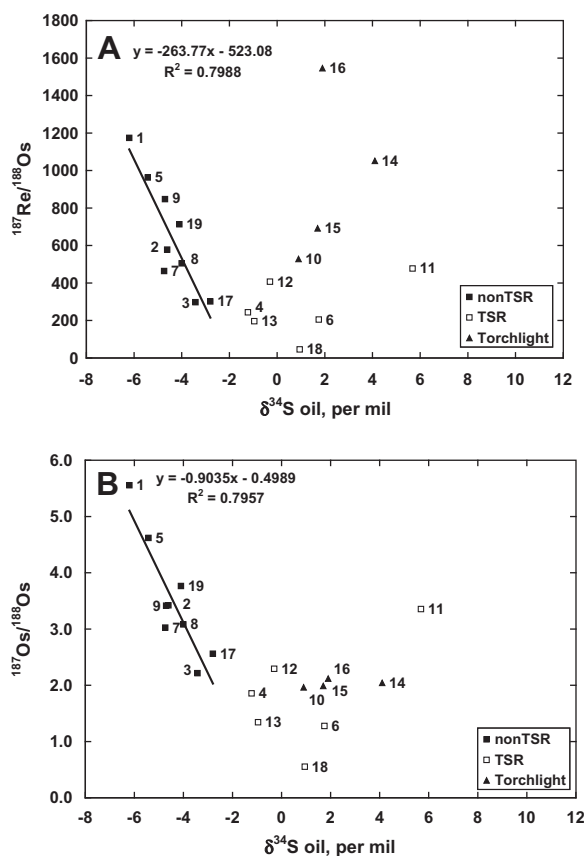


Fig. 11. Plots of (a)  $^{187}\text{Re}/^{188}\text{Os}$  or (b)  $^{187}\text{Os}/^{188}\text{Os}$  versus  $\delta^{34}\text{S}$  oil of Phosphoria-sourced oils from Bighorn Basin. The inverse linear relationship in non-TSR samples may reflect oil generation maturity, whereas the lack of trend in TSR oils suggests that Re–Os isotopes are disturbed by thermochemical sulfate reduction.

verse trends observed for the non-TSR oils is unknown, but one explanation is that it represents a maturity trend for oil generation. The  $\delta^{34}\text{S}$  value of unaltered oil primarily reflects the composition of the source kerogen, and thus has been useful for oil–source rock correlation studies (e.g., Thode, 1981; Orr, 1986; Cai et al., 2009). However, closed system

pyrolysis of kerogen shows up to approximately 2‰ increase of  $\delta^{34}\text{S}$  values in pyrolysates (Idiz et al., 1990; Amrani et al., 2005) and open-system experiments show up to 8‰ increase (Aizenshtat and Amrani 2004). The  $\delta^{34}\text{S}$  trend of oil is not likely due to thermal cracking in the reservoir (Thode et al., 1958; Thode and Monster 1970; Orr, 1974; Aizenshtat and Amrani 2004). Because both the  $^{187}\text{Re}/^{188}\text{Os}$  and  $^{187}\text{Os}/^{188}\text{Os}$  values may be a function of thermal maturity related to oil generation, the main-trend regression (Fig. 4) may represent an interval of time, i.e., the duration of oil generation, rather than a single event.

Orr (1974) proposed that bacterial sulfate reduction (BSR) has occurred in four fields in the Bighorn Basin based on the dissolved sulfate in waters from these fields showing  $\delta^{34}\text{S}$  enrichment over normal Permian sulfate. BSR in or near a petroleum reservoir could introduce isotopically light sulfur to oil (Manowitz et al., 1990; Cai et al., 2005). However, the  $\delta^{34}\text{S}$  values of those oils range from  $-4.4\text{‰}$  to  $+4.3\text{‰}$  and thus no consistent effect of BSR is reflected as low  $\delta^{34}\text{S}$  values.

To test the effect of TSR on the Re–Os scatter of the main trend (Fig. 4), a series of regressions was determined from  $n = 4$  to  $n = 14$  in the order of increasing  $\delta^{34}\text{S}$  values and evaluated on the basis of their MSWD (Table 4). All regressions that include Hamilton Dome (sample 9) have MSWD values of 1342 and greater. For unknown reasons, this oil is clearly an outlier from the main trend. Excluding Hamilton Dome, the regressions of non-TSR oils ( $\delta^{34}\text{S}$  values ranging from  $-5.43$  to  $-2.8$ ,  $n = 4$  to 8) have much less scatter with MSWD values between 134 and 175 (Table 4). A regression with  $n = 8$  (Fig. 12) yields an age of  $211 \pm 21$  Ma with a MSWD = 148. This strongly suggests that TSR has disrupted the Re–Os systematics causing scatter in the main-trend regression (Fig. 4). However, in the  $n = 9$  regression that includes oil sample 4, the MSWD is 169 suggesting that minor TSR (based on  $\delta^{34}\text{S} = -1.2\text{‰}$ ) may have a minimal effect on Re–Os isotopes.

The revised main-trend regression age of  $211 \pm 21$  Ma (Fig. 12) falls near the earliest of the age range proposed for Phosphoria petroleum generation in previous studies (Late Triassic to Late Cretaceous), and is consistent with the expected timing of bitumen generation, which precedes

Table 4

Regression results of Re–Os isotope data from the main-trend oils from  $n = 4$  to  $n = 14$  in the order of increasing  $\delta^{34}\text{S}$  values, showing significant scatter (high MSWD) from results that include oils altered by thermochemical sulfate reduction (TSR), and all results that include the Hamilton Dome oil (sample 9).

$\delta^{34}\text{S}$ max		no.	Sample number	Ma	Ma $\pm$	MSWD	MSWD + 9
-4.6	Non-TSR	4	1,5,7,2	208	47	161	4304
-4.1	Non-TSR	5	1,5,7,2,19	210	34	175	3324
-4.0	Non-TSR	6	1,5,7,2,19,8	211	24	134	2509
-3.4	Non-TSR	7	1,5,7,2,19,8,3	218	20	137	2022
-2.8	Non-TSR	8	1,5,7,2,19,8,3,17	211	21	148	1703
-1.2	TSR	9	1,5,7,2,19,8,3,17,4	219	24	169	1493
-1.0	TSR	10	1,5,7,2,19,8,3,17,4,13	232	33	1259	1342
-0.3	TSR	11	1,5,7,2,19,8,3,17,4,13,12	235	34	1196	2189
1.0	TSR	12	1,5,7,2,19,8,3,17,4,13,12,18	249	35	1096	2006
1.7	TSR	13	1,5,7,2,19,8,3,17,4,13,12,18,6	254	34	1029	1847
5.7	TSR	14	1,5,7,2,19,8,3,17,4,13,12,18, 6,11	254	37	947	1725

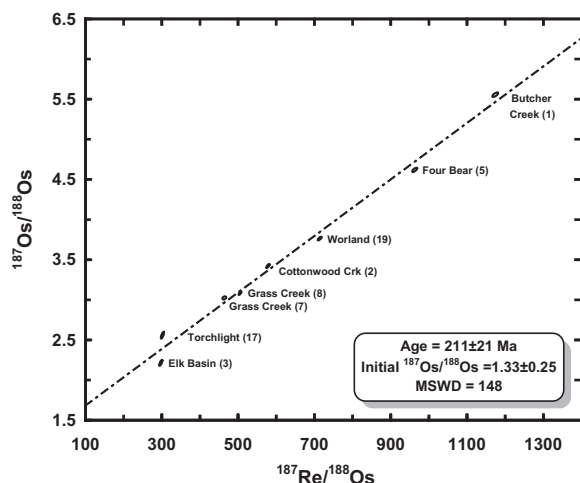


Fig. 12. Re–Os isotope data of Phosphoria-sourced oils from the revised main trend, Bighorn Basin, showing the calculated regression age with reduced scatter (lower MSWD) by excluding oils altered by thermochemical sulfate reduction. Data-point ellipses show the 2-sigma error. Data labels are field names and sample numbers listed on Table 1.

oil generation (Lewan, 1985). However, the process by which oil generation resets the Re–Os isotope systematics remains unclear. The low precision of the regression ( $\pm 21$  Ma) is perhaps the best that could be expected for a generation age given the long duration of generation from the large geographic area of the Phosphoria petroleum system source kitchen, and the possible variations in the initial  $^{187}\text{Os}/^{188}\text{Os}$  values of the Meade Peak and Retort source units. Effects of re-migration also may have also contributed to the scatter but as noted earlier, thermal cracking and biodegradation likely have had minimal or no effect on the main-trend regression.

## 5.2. Re–Os isochron of the Torchlight trend oils

The Torchlight trend (Fig. 3) consists of three oil samples from the Torchlight field (Phosphoria and Madison reservoirs) and one oil from adjacent Lamb field that reside along the eastern margin of the Bighorn Basin (Fig. 1). This trend yields a precise Re–Os isochron of Miocene age ( $9.24 \pm 0.39$  Ma) (Fig. 5). Bjorøy et al. (1996) interpreted the Torchlight oils in Phosphoria and Tensleep reservoirs to be altered by TSR based on high dibenzothiophene and TAS ratios. We also interpret that the Torchlight trend oils have experienced TSR, based on high  $\delta^{34}\text{S}$  values (Fig. 6). One-dimensional burial-history models in the Bighorn Basin show that major uplift and erosion (up to 6500 feet) began at about 10 Ma (Roberts et al., 2008). Subsequent reservoir cooling occurred in reservoirs of the Torchlight trend and most other fields along the margins of the basin. Thus the Miocene-age isochron of the Torchlight trend (Fig. 5) may represent the timing of the end of TSR due to reservoir cooling from uplift and erosion. Other fields in the basin with TSR-altered oil may show Miocene-age isochrons if multiple samples from the same field are obtained (e.g., Torchlight field) that reflect that field's

cooling event. Because Torchlight field is the only field with multiple samples, there remains some uncertainty regarding inter-field versus intra-field variability.

Stone (2004) discounted TSR in Torchlight field and proposed that Torchlight oils in Phosphoria and Tensleep reservoirs contain locally-derived Phosphoria oil generated at the latest stages of the Laramide orogeny (Eocene). One-dimensional burial-history modeling of Phosphoria oil generation in the deeper portions of the Bighorn Basin yield Paleocene generation ages (Heasler et al., 1996; Roberts et al., 2008). Assuming that Phosphoria source rocks exist locally, the timing of generation (Paleocene or Eocene) is inconsistent with the Miocene age recorded by the Torchlight trend isochron.

The existence of Phosphoria source rocks located in the deep portions of the basin in a position to charge Torchlight field is unknown. Maughan (1975) reported Phosphoria outcrop samples of non-source quality from the southern margin of the basin with total organic carbon content less than 1 wt.%. The only oil-prone Phosphoria in the Bighorn Basin that we are aware of comes from a few core samples in wells along the western margin of the basin (USGS unpublished data). Interestingly, slight genetic differences in the Torchlight trend oil biomarker composition (e.g.,  $\text{C}_{26}$  tricyclic/ $\text{C}_{24}$  tetracyclic values, Table 3) are recognized that are suggestive of, but do not require, local sourcing.

The mechanism for effects of TSR on Re–Os systematics is unclear. Although thermal maturation of organic-rich source rocks does not affect the ability of the Re–Os chronometer to yield a precise depositional age for such rocks (Creaser et al., 2002; Selby and Creaser, 2005a), other studies have shown that low temperature (about 100 °C) hydrothermal fluids can disturb Re–Os systematics of organic-rich sedimentary rocks (Kendall et al., 2009b; Rooney et al., 2011) and oil accumulations (Finlay et al., 2010). We suggest that the temperature and chemistry of TSR fluids provide conditions that deplete the organophilic and chalcophilic Re and Os residing in organosulfur ligands in oil by the oxidation of the ligands, or enrich Re and Os in the oil as new organosulfur ligands are generated from back-reacting hydrogen sulfide. Most of the oils altered by TSR are depleted in Re and Os relative to non-TSR oils (Table 2), whereas the Torchlight trend oils (especially samples 14 and 16) are enriched, especially in rhenium. If Re–Os isotopes are indeed shown to be reset by TSR of petroleum, Re–Os geochronology may find future applications in the timing of ore deposits involving thermochemical sulfate reduction in organic-rich sediments.

## 5.3. Mechanism for the formation of a Re–Os isochron in crude oil

The mechanism for the formation of a Re–Os isochron in crude oil has eluded geochemists ever since the phenomenon was first applied to the giant oil-sand deposits of Alberta, Canada (Selby and Creaser, 2005b). They proposed that the process of oil migration homogenizes any differences in both the  $^{187}\text{Re}/^{188}\text{Os}$  and  $^{187}\text{Os}/^{188}\text{Os}$  values, effectively resetting the isotopic chronometer at that time.

However, another mechanism is needed to create the observed range in the  $^{187}\text{Re}/^{188}\text{Os}$  values of an oil family that has allowed construction of reliable isochrons in previous studies. The search for a mechanism must consider that petroleum generation is not instantaneous, but represents an interval of geologic time (e.g., typically >1 m.y.). Therefore a single initial  $^{187}\text{Os}/^{188}\text{Os}$  value is unlikely and a true isochron cannot be constructed for a family of crude oils generated over a wide age range. In this study, covariance of Re and Os isotopes with non-radiogenic parameters such as  $\delta^{34}\text{S}$  oil values (Fig. 11a and b) as well as with  $\delta^{13}\text{C}$  saturated hydrocarbon values and some biomarker parameters of the non-TSR oils (Table 3) reflects the petroleum generation process over an interval of time.

Using hydrous pyrolysis experiments on the Phosphoria Formation, Lewan (1985) showed that petroleum generation is a two-step process in which bitumen is generated from kerogen in the source rock, followed by oil generation from bitumen. From these experiments he derived the kinetics of oil generation, but not bitumen generation. The Re–Os age of Phosphoria oils in this study (Fig. 12) is near the earliest of the age range proposed for Phosphoria petroleum generation in previous studies, and is consistent with the expected timing of bitumen generation. Rhenium and Os reside predominantly in the asphaltene fraction of oil (Selby et al., 2007), and asphaltenes are generated early in petroleum formation when bitumen is generated from kerogen (Lewan, 1985, 1997). More recent hydrous pyrolysis experiments on the Phosphoria Formation (Rooney et al., 2012; 250–325 °C experiments in their Table 4) show that generated bitumen contains more than threefold higher  $^{187}\text{Re}/^{188}\text{Os}$  values than the source rock, whereas  $^{187}\text{Os}/^{188}\text{Os}$  values change very little. If Re–Os isotopes are reset during bitumen generation from kerogen, an oil isochron would record a process that occurs earlier and possibly over a narrower time duration than the process of oil generation from bitumen.

The mechanism for the formation of a Re–Os isotopic relationship in a family of crude oils may involve multiple steps in the petroleum generation process. Bitumen generation from the source rock kerogen may effectively reset the isotopic chronometer by resetting the  $^{187}\text{Re}/^{188}\text{Os}$  isotopic composition while transferring unchanged the  $^{187}\text{Os}/^{188}\text{Os}$  isotopic composition of the kerogen at the time of bitumen generation. Incremental expulsion of oil over the duration of the oil window may provide some of the variation seen in  $^{187}\text{Re}/^{188}\text{Os}$  values from an oil family.

## 6. CONCLUSIONS

Crude oils from the Bighorn Basin of Wyoming and Montana selected for this study are interpreted to be derived from the Permian Phosphoria Formation based on oil–oil and oil–source rock correlations. An oil from Butcher Creek field is a biodegraded Phosphoria-sourced oil that has a second charge of high-gravity oil of unknown (possibly Cretaceous) source. Most Phosphoria-sourced oils have  $\delta^{34}\text{S}$  values between  $-7\text{‰}$  and  $-2\text{‰}$ , whereas oils from the Bighorn Basin range from  $-6.2\text{‰}$  to  $+5.7\text{‰}$ . Some of the oils along the eastern margin of the basin are isotopically

heavier (greater than  $-2\text{‰}$ ) due to alteration in the reservoir by thermochemical sulfate reduction (TSR).

The Re and Os isotope data of the Phosphoria oils plot in two general trends with the main-trend oils ( $n = 15$ ) yielding a Triassic age ( $239 \pm 43$  Ma) with an initial  $^{187}\text{Os}/^{188}\text{Os}$  value of  $0.85 \pm 0.42$  and a MSWD of 1596, and the Torchlight trend oils ( $n = 4$ ) yielding an isochron of Miocene age ( $9.24 \pm 0.39$  Ma) with an initial  $^{187}\text{Os}/^{188}\text{Os}$  value of  $1.88 \pm 0.01$  and a MSWD of 0.05. The scatter in the regression of the main-trend oils is likely due to several factors including petroleum alteration due to TSR. A revised regression of the main-trend oils that excludes the TSR-altered oils yields an age of  $211 \pm 21$  Ma with significantly reduced scatter (MSWD of 148).

This revised age ( $211 \pm 21$  Ma) is consistent with the expected timing of bitumen generation or the beginning of oil generation, and does not seem to reflect the source rock age (Permian,  $\sim 270$  Ma) or the timing of re-migration (Late Cretaceous to Eocene,  $\sim 70$ – $50$  Ma) associated with the Laramide orogeny. The low precision of the revised regression ( $\pm 21$  Ma;  $\sim 10\%$ ) is not unexpected for this family of crude oils given the long duration ( $>70$  m.y.) of generation from the large geographic area of the Phosphoria petroleum system source kitchen, and the possible variations over 5 m.y. in the initial  $^{187}\text{Os}/^{188}\text{Os}$  value of the Meade Peak and Retort source units within the Phosphoria Formation. In-reservoir thermal cracking, biodegradation, and water washing have minimal or no apparent effect on the main-trend regression.

The Phosphoria-sourced oil samples from Torchlight and Lamb field (Torchlight trend) yield a precise Miocene age Re–Os isochron. The Miocene age may reflect the end of TSR in the Torchlight field reservoir rock due to cooling below a threshold temperature in the last 10 m.y. due to uplift and erosion of the overlying rocks. A 3-D burial history model of the Bighorn Basin that includes both the kinetics of petroleum generation and thermochemical sulfate reduction might explain the Miocene Torchlight trend isochron, and identify potential oil accumulations that are derived from local Phosphoria sources.

The mechanism for the formation of a Re–Os isotope relationship in a family of crude oils may involve multiple steps in the petroleum generation process. Bitumen generation may provide a reset of the isotopic chronometer, and incremental expulsion of oil over the duration of the oil window may provide some of the variation seen in  $^{187}\text{Re}/^{188}\text{Os}$  values from an oil family.

## ACKNOWLEDGMENTS

We thank the U.S. Geological Survey Energy Resources Program organic geochemistry laboratory personnel, Zach Lowry, Augusta Warden, Tammy Hanna, Mark Drier, and Robert Dias, for providing all geochemical analyses except Re–Os (Selby) and S isotopes (Cayce Gulbransen, USGS). Several operators granted permission to sample oil production including Marathon Oil Co., Carol Holly Oil Corp., Rock Well Petroleum, Cody Petroleum, Devon Energy, Wyoil Corp., KCS Mountain Resources, Saga Petroleum, and Citation Oil and Gas. Don Stone provided some of the oils from Torchlight field and some insights on the geology of the Bighorn Basin. This paper benefited greatly from construc-

tive reviews by Bernard Bingen, Joseph Curiale, and Michael Lewan, and editorial assistance by David Ferderer and Tom Judkins. Any use of trade, firm, or product names is for descriptive purposes only and does not imply endorsement by the U.S. Government.

## REFERENCES

- Aizenshtat Z. and Amrani A. (2004) Significance of  $\delta^{34}\text{S}$  and evaluation of its imprint on sedimentary sulfur rich organic matter II: thermal changes of kerogens type II -S catagenetic stage controlled mechanisms. A study and conceptual overview. In *Geochemical Investigations in Earth and Space Science: A Tribute to Isaac R. Kaplan* (eds. R. J. Hill, J. Leventhal, Z. Aizenshtat, M. J. Baedeker, G. Claypool, R. Eganhouse, M. Goldhaber and K. Peters). The Geochemical Society, Publication No. 9, pp. 35–50.
- Amrani A., Lewan M. D. and Aizenshtat Z. (2005) Stable sulfur isotope partitioning during simulated petroleum formation as determined by hydrous pyrolysis of Ghareb Limestone, Israel. *Geochim. Cosmochim. Acta* **69**, 5317–5331.
- Ault W. U. and Kulp J. L. (1959) Isotopic geochemistry of sulphur. *Geochim. Cosmochim. Acta* **16**, 201–235.
- Barbat W. N. (1967) Crude-oil correlations and their role in exploration. *AAPG Bull.* **51**, 1255–1292.
- Bjorøy M., Williams J. A., Dolcater D. L., Kemp M. K. and Winters J. C. (1996) Maturity assessment and characterization of Big Horn Basin Palaeozoic oils. *Mar. Pet. Geol.* **13**, 3–23.
- Burtner R. L. and Nigrini A. (1994) Thermochronology of the Idaho–Wyoming thrust belt during the Sevier Orogeny: a new, calibrated, multiprocess thermal model. *AAPG Bull.* **78**, 1586–1612.
- Cai C. F., Worden R. H., Wolff G. A., Bottrell S. H., Wang D. L. and Li X. (2005) Origin of sulfur rich oils and  $\text{H}_2\text{S}$  in Tertiary lacustrine sections of the Jinxian Sag, Bohai Bay Basin, China. *Appl. Geochem.* **20**, 1427–1444.
- Cai C. F., Zhang C. M., Cai L., Wu G. H., Jiang L., Xu Z., Li K., Ma A. L. and Chen L. X. (2009) Origins of Paleozoic oils in the Tarim Basin: evidence from sulfur isotopes and biomarkers. *Chem. Geol.* **268**, 197–210.
- Campbell C. V. (1956) The Phosphoria Formation in the Southeastern Bighorn Basin, Wyoming. Ph. D. thesis, Stanford Univ.
- Campbell C. V. (1962) Depositional environments of Phosphoria Formation (Permian) in southeastern Bighorn Basin, Wyoming. *AAPG Bull.* **46**, 478–503.
- Cheney T. M. and Sheldon R. P. (1959) Permian stratigraphy and oil potential, Wyoming and Utah. In *Intermountain Association of Petroleum Geologists 10th Annual Field Conference*. Intermountain Association of Petroleum Geologists, pp. 90–100.
- Chung H. M., Brand S. W. and Grizzle P. L. (1981) Carbon isotope geochemistry of Paleozoic oils from Big Horn Basin. *Geochim. Cosmochim. Acta* **45**, 1803–1815.
- Claypool G. E. and Mancini E. A. (1989) Geochemical relationships of petroleum in Mesozoic reservoirs to carbonate source rocks of Jurassic Smackover Formation, Southwestern Alabama. *AAPG Bull.* **73**, 904–924.
- Claypool G. E., Love A. H. and Maughan E. K. (1978) Organic geochemistry, incipient metamorphism, and oil generation in black shale members of Phosphoria Formation, Western Interior United States. *AAPG Bull.* **62**, 98–120.
- Clayton C. J. (1991) Effect of maturity on carbon isotope ratios of oils and condensates. *Org. Geochem.* **17**, 887–899.
- Cohen A. S., Coe A. L., Bartlett J. M. and Hawkesworth C. J. (1999) Precise Re–Os ages of organic-rich mudrocks and the Os isotope composition of Jurassic seawater. *Earth Planet. Sci. Lett.* **167**, 159–173.
- Creaser R. A., Sannigrahi P., Chacko T. and Selby D. (2002) Further evaluation of the Re–Os geochronometer in organic-rich sedimentary rocks: a test of hydrocarbon maturation effects in the Exshaw Formation, Western Canada Sedimentary Basin. *Geochim. Cosmochim. Acta* **66**, 3441–3452.
- Cumming V. M., Selby D. and Lillis P. G. (2012) Re–Os geochronology of the lacustrine Green River Formation: insights into direct depositional dating of lacustrine successions, Re–Os systematics and paleocontinental weathering. *Earth Planet. Sci. Lett.* **359–360**, 194–205.
- Dahl J., Moldowan J. M. and Sundararaman P. (1993) Relationship of biomarker distribution to depositional environment: Phosphoria Formation, Montana, U.S.A. *Org. Geochem.* **20**, 1001–1017.
- Edman J. D. and Surdam R. C. (1984) Influence of overthrusting on maturation of hydrocarbons in Phosphoria Formation, Wyoming–Idaho–Utah overthrust belt. *AAPG Bull.* **68**, 1803–1817.
- Eglinton T. I., Sinnighe Damste J. S., Kohnen M. E. L. and de Leeuw J. W. (1990) Rapid estimation of the organic sulphur content of kerogens, coals and asphaltenes by pyrolysis–gas chromatography. *Fuel* **69**, 1394–1404.
- Finlay A. J., Selby D., Osborne M. J. and Finucane D. (2010) Fault-charged mantle-fluid contamination of United Kingdom North Sea oils: insights from Re–Os isotopes. *Geology* **28**, 979–982.
- Finlay A. J., Selby D. and Osborne M. J. (2011) Re–Os geochronology and fingerprinting of United Kingdom Atlantic margin oil: temporal implications for regional petroleum systems. *Geology* **39**, 475–478.
- Fox J. E. and Dolton G. L. (1996) Bighorn Basin Province (034). In *1995 National Assessment of United States Oil and Gas Resources—Digital Map Data, Text, and Graphical Images* (compilers, W. R. Beeman, R. C. Obuch and J. D. Brewton). U.S. Geological Survey Digital Data Series DDS-35, CD-ROM.
- Georgiev S., Stein H., Hannah J., Bingen B., Weiss H. M. and Piasecki S. (2011) Hot acidic Late Permian seas stifled life in record time. *Earth Planet. Sci. Lett.* **310**, 389–400.
- Giesemann A., Jäger H. J., Norman A. L., Krouse H. R. and Brand W. A. (1994) On-line sulfur-isotope determination using an elemental analyzer coupled to a mass spectrometer. *Anal. Chem.* **66**, 2816–2819.
- Goldstein T. P. and Aizenshtat Z. (1994) Thermochemical sulfate reduction – a review. *J. Therm. Anal.* **42**, 241–290.
- Gradstein F. M., Ogg J. G., Smith A. G., Bleeker W. and Lourens L. J. (2004) A new Geologic Time Scale, with special reference to Precambrian and Neogene. *Episodes* **27**(2), 83–100.
- Heasler H. P., Visser N., Kharitonova N. A. and Surdam R. C. (1996) Thermal effects of rapid sedimentation and uplift on the maturation of hydrocarbons in the Bighorn Basin, Wyoming. In *Resources of the Bighorn Basin – 47th Annual Field Conference Guidebook*. Wyoming Geological Association, pp. 41–57.
- Idiz E. F., Tannenbaum E. and Kaplan I. R. (1990) Pyrolysis of high-sulfur Monterey kerogens. In *Geochemistry of Sulfur in Fossil Fuels*, vol. 429 (eds. W. L. Orr and C. M. White). American Chemical Society Symposium Series, pp. 575–591.
- Kendall B., Creaser R. A. and Selby D. (2009a)  $^{187}\text{Re}$ – $^{187}\text{Os}$  geochronology of Precambrian organic-rich sedimentary rocks. *Geol. Soc. London Spec. Publ.* **326**, 85–107.
- Kendall B., Creaser R. A., Gordon G. W. and Anbar A. D. (2009b) Re–Os and Mo isotope systematics of black shales from the Middle Proterozoic Velkerri and Wollgorang Formations,

- McArthur Basin, northern Australia. *Geochim. Cosmochim. Acta* **73**, 2534–2558.
- Kirschbaum M. A., Lillis P. G. and Roberts L. N. R. (2007) Geologic assessment of undiscovered oil and gas resources in the Phosphoria total petroleum system of the Wind River Basin Province, Wyoming. In *Petroleum Systems and Geologic Assessment of Oil and Gas in the Wind River Basin Province, Wyoming*. U.S. Geological Survey Digital Data Series DDS-69-J, Chapter 3, 27p.
- Kirschbaum M. A., Condon S. M., Finn T. M., Johnson R. C., Lillis P. G., Nelson P. H., Roberts L. N. H., Roberts S. B., Charpentier R. R., Cook T. A., Klett T. R., Pollastro R. M. and Schenk C. J. (2008) Assessment of Undiscovered Oil and Gas Resources of the Bighorn Basin Province, Wyoming and Montana, 2008. *U.S. Geological Survey Fact Sheet FS-2008-3050*, 2p.
- Kuo L. (1994) An experimental study of crude oil alteration in reservoir rocks by water washing. *Org. Geochem.* **21**, 465–479.
- Lafargue E. and Barker C. (1988) Effect of water washing on crude oil compositions. *AAPG Bull.* **72**, 263–276.
- Larter S. R. and Aplin A. C. (1995) Reservoir geochemistry: methods, applications and opportunities. In *The Geochemistry of Reservoirs* (eds. J. M. Cubitt and W. A. England). Geological Society Special Publication No. 86, Geological Society, London, pp. 5–32.
- Lewan M. D. (1985) Evaluation of petroleum generation by hydrous pyrolysis experimentation. *Philos. Trans. R. Soc. Lond. A* **315**, 123–134.
- Lewan M. D. (1997) Experiments on the role of water in petroleum formation. *Geochim. Cosmochim. Acta* **61**, 3691–3723.
- Lewan M. D., Bjørøy M. and Dolcater D. L. (1986) Effects of thermal maturation on steroid hydrocarbons as determined by hydrous pyrolysis of the Phosphoria Retort Shale. *Geochim. Cosmochim. Acta* **50**, 1977–1987.
- Lillis P. G., Warden A. and King J. D. (2003) Petroleum systems of the Uinta and Piceance Basins—geochemical characteristics of oil types, Chapter 3. In *Petroleum Systems and Geologic Assessment of Oil and Gas in the Uinta-Piceance Province, Utah and Colorado*. U.S. Geological Survey Digital Data Series DDS-69-B, 25p.
- Ludwig K. R. (2009) Isoplot, a plotting and regression program for radiogenic-isotope data, version 3.72. Berkeley Geochronology Center, Berkeley, California, <[http://www.bgc.org/isoplot\\_etc/isoplot.html](http://www.bgc.org/isoplot_etc/isoplot.html)>.
- Machel H. G. (2001) Bacterial and thermochemical sulfate reduction in diagenetic settings – old and new insights. *Sed. Geol.* **140**, 143–175.
- Machel H. G., Krouse H. R. and Sassen R. (1995) Products and distinguishing criteria of bacterial and thermochemical sulfate reduction. *Appl. Geochem.* **10**, 373–389.
- Manowitz B., Krouse H. R., Barker C. and Premuzic E. T. (1990) Sulfur isotope data analysis of crude oils from the Bolivar Coastal Fields (Venezuela). In *Geochemistry of Sulfur in Fossil Fuels*, vol. 429 (eds. W. L. Orr and C. M. White). American Chemical Society Symposium Series, pp. 592–612.
- Manzano B. K., Fowler M. G. and Machel H. G. (1997) The influence of thermochemical sulphate reduction on hydrocarbon composition in Nisku reservoirs, Brazeau River area, Alberta, Canada. *Org. Geochem.* **27**, 507–521.
- Maughan, E. K. (1975) Organic carbon in shale beds of the Permian Phosphoria Formation of eastern Idaho and adjacent states – a summary report. In *Geology and Mineral Resources of the Bighorn Basin — 27th Annual Field Conference Guidebook*. Wyoming Geological Association, pp. 107–115.
- Maughan E. K. (1984) Geological setting and some geochemistry of petroleum source rocks in the Permian Phosphoria Formation. In *Hydrocarbon Source Rocks of the Greater Rocky Mountain region* (eds. J. Woodward, F. F. Meissner and J. L. Clayton). Rocky Mountain Association of Geologists, pp. 281–294.
- NIPER (1995) National Institute for Petroleum and Energy Research crude oil analysis database. National Energy Technology Laboratory, Department of Energy. <<http://www.netl.doe.gov/technologies/oil-gas/Software/database.html>> (accessed 2007).
- Orr W. L. (1974) Changes in sulfur content and isotopic ratios of sulfur during petroleum maturation— study of Big Horn Basin Paleozoic oils. *AAPG Bull.* **58**, 2295–2318.
- Orr W. L. (1986) Kerogen/asphaltene/sulfur relationships in sulfur-rich Monterey oils. *Org. Geochem.* **10**, 499–516.
- Orr W. L. (2001) Evaluating kerogen sulfur content from crude oil properties—Cooperative Monterey organic geochemistry study. In *The Monterey Formation—from Rocks to Molecules* (eds. C. M. Isaacs and J. Rullkötter). Columbia University Press, New York, pp. 348–367.
- Orr W. L. and Sinninghe Damste J. S. (1990) Geochemistry of sulfur in petroleum systems. In *Geochemistry of Sulfur in Fossil Fuels*, vol. 429 (eds. W. L. Orr and C. M. White). American Chemical Society Symposium Series, pp. 2–29.
- Palmer S. E. (1984) Effect of water washing on C<sub>15+</sub> hydrocarbon fraction of crude oils from northwest Palawan, Philippines. *AAPG Bull.* **68**, 137–149.
- Peters K. E., Walters C. C. and Moldowan J. M. (2005) *The Biomarker Guide*, second ed. Cambridge University Press, 1155p.
- Peterson J. A. (1984) Permian stratigraphy, sedimentary facies, and petroleum geology, Wyoming, and adjacent area. In *Thirty-Fifth Annual Field Conference – 1984, Wyoming Geological Association Guidebook*. pp. 25–64.
- Peterson F. (1988) Pennsylvanian to Jurassic eolian transportation systems in the western United States. *Sed. Geol.* **56**, 207–260.
- Peucker-Ehrenbrink B. and Ravizza G. (2000) The marine osmium isotope record. *Terra Nova* **12**, 205–219.
- Piper D. Z. and Link P. K. (2002) An upwelling model for the Phosphoria sea: a Permian, ocean-margin sea in the northwest United States. *AAPG Bull.* **86**, 1217–1235.
- Price L. C. (1980) Utilization and documentation of vertical oil migration in deep basins. *J. Petrol. Geol.* **2**, 353–387.
- Price L. C. (1997) Origins, characteristics, evidence for, and economic viabilities of conventional and unconventional gas resource bases. In *Geologic Controls of Deep Natural Gas Resources in the United States*. U.S. Geological Survey Bulletin 2146-L.
- Price L. C. and Wenger L. M. (1992) The influence of pressure on petroleum generation and maturation as suggested by aqueous pyrolysis. *Org. Geochem.* **19**, 141–159.
- Ravizza G. and Turekian K. K. (1989) Application of the <sup>187</sup>Re <sup>187</sup>Os system to black shale geochronometry. *Geochim. Cosmochim. Acta* **53**, 3257–3262.
- Roberts L. N. R., Lewan M. D. and Finn T. M. (2004) Timing of oil and gas generation of petroleum systems in the Southwestern Wyoming Province. *Mt. Geol.* **41**, 87–118.
- Roberts L. N. R., Finn T. M., Lewan M. D. and Kirschbaum M. A. (2008) Burial history, thermal maturity, and oil and gas generation history of source rocks in the Bighorn Basin, Wyoming and Montana. *U.S. Geological Survey Scientific Investigations Report 2008–5037*. 28p.
- Rooney A. D., Selby D., Houzay J.-P. and Renne P. R. (2010) Re–Os geochronology of a Mesoproterozoic sedimentary succession, Taoudeni basin, Mauritania: implications for basin-wide correlations and Re–Os organic-rich sediments systematics. *Earth Planet. Sci. Lett.* **289**, 486–496.

- Rooney A. D., Chew D. M. and Selby D. (2011) Re–Os geochronology of the Neoproterozoic–Cambrian Dalradian Supergroup of Scotland and Ireland: implications for Neoproterozoic stratigraphy, glaciations and Re–Os systematics. *Precambr. Res.* **185**, 202–214.
- Rooney A. D., Selby D., Lewan M. D., Lillis P. G. and Houzay Jean-Pierre (2012) Evaluating Re–Os systematics in organic-rich sedimentary rocks in response to petroleum generation using hydrous pyrolysis experiments. *Geochim. Cosmochim. Acta* **77**, 275–291.
- Selby D. and Creaser R. A. (2005a) Direct radiometric dating of the Devonian–Mississippian time-scale boundary using the Re–Os black shale geochronometer. *Geology* **33**, 545–548.
- Selby D. and Creaser R. A. (2005b) Direct radiometric dating of hydrocarbon deposits using rhenium–osmium isotopes. *Science* **308**, 1293–1295.
- Selby D., Creaser R. A., Dewing K. and Fowler M. (2005) Evaluation of bitumen as a  $^{187}\text{Re}$ – $^{187}\text{Os}$  geochronometer for hydrocarbon maturation and migration: a test case from the Polaris MVT deposit, Canada. *Earth Planet. Sci. Lett.* **235**, 1–15.
- Selby D., Creaser R. A. and Fowler M. (2007) Re–Os elemental and isotopic systematics in crude oils. *Geochim. Cosmochim. Acta* **71**, 378–386.
- Sheldon R. P. (1963) Physical stratigraphy and mineral resources of Permian Rocks in Western Wyoming. *U.S. Geological Survey Professional Paper 313-B*, 273p.
- Sheldon R. P. (1967) Long-distance migration of oil in Wyoming. *Miner. Resour. Dev. Ser.* **26**, 113–117.
- Silliman J. E., Li M., Yao H. and Hwang R. (2002) Molecular distributions and geochemical implications of pyrrolic nitrogen compounds in the Permian Phosphoria Formation derived oils of Wyoming. *Org. Geochem.* **33**, 527–544.
- Sinninghe Damsté J. S., Eglinton T. I., de Leeuw J. W. and Schenck P. A. (1989) Organic sulphur in macromolecular sedimentary organic matter: I. Structure and origin of sulphur-containing moieties in kerogen, asphaltenes and coal as revealed by flash pyrolysis. *Geochim. Cosmochim. Acta* **53**, 873–889.
- Smoliar M. I., Walker R. J. and Morgan J. W. (1996) Re–Os isotope constraints on the age of Group IIA, IIIA, IVA, and IVB iron meteorites. *Science* **271**, 1099–1102.
- Sofer Z. (1984) Stable carbon isotope compositions of crude oils: application to source depositional environments and petroleum alteration. *AAPG Bull.* **68**, 31–49.
- Stone D. S. (1967) Theory of Paleozoic oil and gas accumulation in Big Horn basin, Wyoming. *AAPG Bull.* **51**, 2056–2114.
- Stone D. S. (1996) Fourbear field: an Eocene laccofold, western Bighorn Basin. In *Resources of the Bighorn Basin, 47th Annual Field Conference Guidebook* (eds. C. E. Bowen, S. C. Kirkwood and T. S. Miller). Wyoming Geological Survey, pp. 69–92.
- Stone D. S. (2004) Rio thrusting, multi-stage migration, and formation of vertically segregated Paleozoic oil pools at Torchlight field on the Greybull Platform (Eastern Bighorn Basin): implications for exploration. *Mt. Geol.* **41**, 119–138.
- Thode H. G. (1981) Sulfur isotope ratios in petroleum research and exploration: Williston Basin. *AAPG Bull.* **65**, 1527–1535.
- Thode H. G. and Monster J. (1970) Sulfur isotope abundances and genetic relations of oil accumulations in Middle East Basin. *AAPG Bull.* **54**, 627–637.
- Thode H. G., Monster J. and Dunford H. B. (1958) Sulphur isotope abundances in petroleum and associated materials. *AAPG Bull.* **42**, 2619–2641.
- Tissot B. P. and Welte D. H. (1984) *Petroleum Formation and Occurrence*, Second Revised and Enlarged Edition. Springer-Verlag, Berlin, 699p.
- Tsuzuki N., Takeda N., Suzuki M. and Yokoi K. (1999) The kinetic modeling of oil cracking by hydrothermal pyrolysis experiments. *Int. J. Coal Geol.* **39**, 227–250.
- Turgeon S. C. and Creaser R. A. (2008) Cretaceous oceanic anoxic event 2 triggered by a massive magmatic episode. *Nature* **454**, 323–327.
- Vredenburg L. D. and Cheney E. S. (1971) Sulfur and carbon isotopic investigation of petroleum, Wind River Basin, Wyoming. *AAPG Bull.* **55**, 1954–1975.
- Xu G., Hanna J. L., Stein H. J., Bingen B., Yang G., Zimmerman A., Weitschat W., Mork A. and Weiss H. M. (2009) Re–Os geochronology of Arctic black shales to evaluate the Anisian–Ladinian boundary and global faunal correlations. *Earth Planet. Sci. Lett.* **288**, 581–587.
- Zhang T., Ellis G. S., Wang K., Walters C. C., Kelemen S. R., Gillaizeau B. and Tang Y. (2007) Effect of hydrocarbon type on thermochemical sulfate reduction. *Org. Geochem.* **38**, 897–910.
- Zhang T., Ellis G. S., Walters C. C., Kelemen S. R., Wang K. and Tang Y. (2008) Geochemical signatures of thermochemical sulfate reduction in controlled hydrous pyrolysis experiments. *Org. Geochem.* **39**, 308–328.

Associate editor: Marc Norman